Rigorous upscaling of rough boundaries for reactive flows

EINDHOVEN UNIVERSITY OF TECHNOLOGY
Department of Mathematics and Computer Science

CASA-Report 12-37
October 2012

Rigorous upscaling of rough boundaries for reactive flows

by

K. Kumar, M. van Helvoort, I.S. Pop

Centre for Analysis, Scientific computing and Applications
Department of Mathematics and Computer Science
Eindhoven University of Technology
P.O. Box 513
5600 MB Eindhoven, The Netherlands
ISSN: 0926-4507

Rigorous upscaling of rough boundaries for reactive flows

K. Kumar[1], **M. van Helvoort** [1], **and I. S. Pop**[1]

[1] Department of Mathematics and Computer Sciences, Eindhoven University of Technology, 5600 MB, Eindhoven, The Netherlands

Key words Reactive flows, rough boundaries, homogenization.

MSC (2000) 35B27,76S05,76V05,76R50

We consider a mathematical model for reactive flow in a channel having a rough (periodically oscillating) boundary with both period and amplitude ε. The ions are being transported by the convection and diffusion processes. These ions can react at the rough boundaries and get attached to form the crystal (precipitation) and become immobile. The reverse process of dissolution is also possible. The model involves non-linear and multi-valued rates. We provide a rigorous justification for the upscaling process in which we define an upscaled problem defined in a simpler domain with flat boundaries. To this aim, we use periodic unfolding techniques combined with translation estimates. Numerical experiments confirm the theoretical predictions and illustrate a practical application of this upscaling process.

1 Introduction

We consider the reactive flow through a channel having rough (periodically oscillating) boundaries. The flow carries the ions/solutes which are transported through the channel by a combined process of diffusion and convection. The modeling of the process therefore consists of transport and flow problems. The ions in the bulk react at the rough boundary and form crystals (hence become immobile). The opposite process of dissolution, that is the ions dissolving in the bulk phase, is also possible. We assume that the thickness of the crystal deposited is small enough so that we ignore the change in the geometry that is due to the chemistry.

As the original problem is defined in a domain with rapidly oscillating boundary, solving it numerically requires resolving these oscillations at sufficient resolution. This implies that the mesh size should be much smaller than the size of oscillations. This makes the problem computationally expensive. Alternatively, one can consider an upscaled model providing an approximation to the original model in a domain with flat boundaries. Of course, this requires taking into account some corrections due to this simplification, which are incorporated in modified boundary conditions. In particular, the flux at the rough boundaries needs to be corrected if we are to simplify the boundary to a flat one. Also, the upscaling process should contain some information from the original geometry. In this work, we justify this upscaling process in a rigorous manner.

We make a specific choice for the reaction rate in this work, describing the crystal precipitation and dissolution processes. The rate description is defined at the boundary and hence on a lower dimensional manifold. Moreover, this rate is the net result of two opposing processes: precipitation and dissolution. The precipitation term is described by a non-linear term while the dissolution term is described by the Heaviside graph resulting in a multi-valued character. These kind of models are well established in literature; for details we refer to [15–17, 41–43]. This specific choice of the reaction rate poses mathematical difficulties and in particular the multi-valued nature of the dissolution term defined at the boundary limits the regularity of the solution.

Homogenization techniques are widely applied for reactive flows. Compactness and 2-scale convergence arguments are successfully employed for perforated domains like porous media, see [1, 22–24, 36, 38–40]. Upscaling of rough boundaries however require slightly different approaches and extensive work has been done in this respect. The elliptic equations defined in domains with rough boundaries have been treated in [2–5, 10, 20, 37]. Also, we refer to [21] for upscaling when geometry changes are taken into account.

Our contributions in this respect are two-fold: first, we consider a model for reactions described by a non-linear, non-Lipschitz ODE at the rough boundary coupled with a parabolic PDE in domain; and secondly, we use periodic unfolding

Corresponding author: Kundan Kumar e-mail: k.kumar@tue.nl.

techniques for deriving effective boundary conditions. This technique has been systematically introduced by [11] (see also [8] for similar ideas) and has been applied for homogenization problems, in particular for periodic homogenization. Relevant references to this work are [32] and [12]. In the former, matched asymptotic techniques are employed to derive formally an effective boundary condition for a similar problem, but in the case when the rough boundaries are also free boundaries and hence the domain changes in time. In the latter, homogeneous boundary conditions are treated for a related but different geometry. The use of periodic unfolding provides a natural framework to deal with upscaling problems by mapping the integrals from $\varepsilon-$dependent geometries to fixed geometries thereby making the use of compactness properties in a fairly evident manner. In this work, we use the periodic unfolding technique to obtain the upscaled problem for the oscillating boundary case. Specifically, we consider the boundary, oscillating with amplitude and period ε. We consider the limit of the problem as $\varepsilon \searrow 0$ and define this limit to be the upscaled problem. As a technical note, the idea is as follows: the system of equations provides a priori estimates in the original domain and at the oscillating boundary. The latter estimates are used to obtain those for the unfolded sequences of the traces. In addition to this, the non-linearities in the reaction rate requires stronger compactness which is achieved by considering translation estimates.

This chapter is structured as follows. We present a brief introduction of the model in Section 2 followed by the definition of upscaled problem in Section 3. The a priori estimates are stated in Section 4 and the derivation of the upscaled equations is completed in Section 5. Note that even though the details of the proof are presented for a particular rate, the techniques presented in this work can be used to treat other cases. We comment on this in Section 6. The numerical computations are discussed in Section 7.

2 Geometry and modeling

First we describe the setting of the geometry in which the physical processes are observed. This will be followed by a brief recall of the model describing the convective and diffusive transport of solutes in the fluid. The present context falls into the general framework of reactive flows in porous media. For the particular description of dissolution and precipitation, we refer to [14–16] for an upscaled (core scale) model. Here we adopt the pore scale counterpart discussed in [17]. The rigorous homogenization procedure from the pore scale model to the core scale model one is proved in [30] .

2.1 Basic geometry

Let $\Omega := (0,1) \times (0,1)$ be the homogenized domain with flat boundaries. The domain with $\varepsilon-$dependent oscillating boundary is defined as follows. Let $h : \Re \mapsto [-1, 0]$ be a given smooth $1-$ periodic function and define

$$h^\varepsilon(x) = \varepsilon h\left(\frac{x}{\varepsilon}\right).$$

Then $\Omega^\varepsilon \subset \Re^2$ with Ω^ε is the open, bounded set

$$\Omega^\varepsilon := \left\{(x,y) \in \Re^2 : x \in (0,1) \quad y \in (h^\varepsilon(x), 1)\right\}.$$

With $\partial\Omega^\varepsilon$ being the boundary of Ω^ε, the oscillating boundary $\Gamma^\varepsilon (\subset \partial\Omega^\varepsilon)$ is defined as:

$$\Gamma^\varepsilon := \left\{(x,y) : x \in (0,1), \quad y = \varepsilon h\left(\frac{x}{\varepsilon}\right)\right\}.$$

Since Γ^ε is periodic, we scale one period and define Γ

$$\Gamma := \{(z,y) : z \in (0,1), \quad y = h\,(z)\}.$$

The inlet and outlet boundaries of Ω^ε are defined as

$$\Gamma_i := \{(x,y) : x = 0,\ h^\varepsilon(0) \le y \le 1\}$$
$$\Gamma_o := \{(x,y) : x = 1,\ h^\varepsilon(0) \le y \le 1\}.$$

This particular scaling for Γ^ε ensures that its $\mathcal{H}^1$ Lebesgue measure remains bounded and is of order $O(1)$. Note that, by construction, we have $\Omega \subset \Omega^\varepsilon$ since $h^\varepsilon \le 0$. We take $\Omega \subset \Omega^\varepsilon$ to avoid extension arguments. The geometry is sketched in Figure 1. Also note that having fixed ε, the domain Ω^ε and the boundary Γ^ε remain fixed as well.

Let T be a given time; we define

$$\Omega^T := (0,T] \times \Omega, \quad \Omega^{\varepsilon T} := (0,T] \times \Omega^\varepsilon, \quad \Gamma^{\varepsilon T} := (0,T] \times \Gamma^\varepsilon.$$

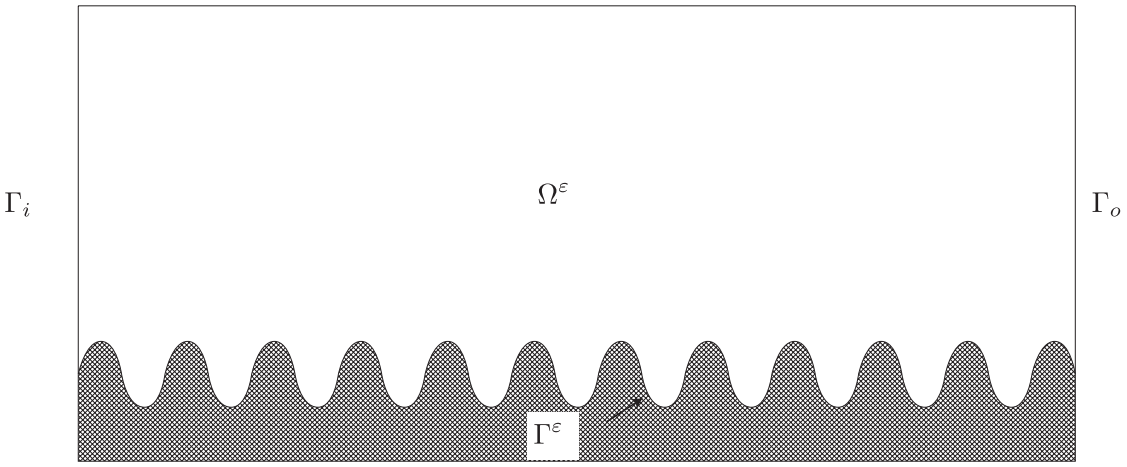

Fig. 1 The domain Ω^ε, and the boundary Γ^ε determined by the periodic function h^ε. Note that both remain fixed in time for a given ε.

As announced before, the solutes in the channel diffuse, are transported by the flow, and react at the rough boundary. To fix the ideas, we assume that the flow is modeled by the Stokes system, where $\mathbf{q}^\varepsilon$ denotes the flow velocity and P^ε its pressure,

$$\left\{ \begin{array}{rcrl} \Delta \mathbf{q}^\varepsilon & = & \nabla P^\varepsilon & \text{in} \quad \Omega^{\varepsilon T}, \\ \nabla \cdot \mathbf{q}^\varepsilon & = & 0 & \text{in} \quad \Omega^{\varepsilon T}. \end{array} \right. \tag{1}$$

Without loss of generality, we have normalized the dynamic viscosity to be 1. For the boundary conditions, we pose a parabolic profile at the inlet,

$$\mathbf{q}^\varepsilon(y) = Q(y - h^\varepsilon(0))(1-y)\mathbf{e}_1 \quad \text{at} \quad \Gamma_i,$$

where $Q > 0$ is a positive constant and $\mathbf{e}_1$ is the unit vector in $x-$direction. For the outlet, we prescribe the pressure. For the other boundaries, including Γ^ε, we impose no-slip boundary conditions. The specific model for $\mathbf{q}^\varepsilon$ considered here is not essential and the results remain valid for other situations.

Next, we consider the model for the transport of solutes which is described by the linear convection-diffusion equation. Under assumed compatibility conditions [15, 16, 29] (e.g. electrical neutrality) it is sufficient to consider only one type of ions. Let u^ε denote the concentration of the ions and v^ε the crystal concentration, the transport equation reads

$$\partial_t u^\varepsilon + \nabla \cdot (\mathbf{q}^\varepsilon u^\varepsilon - \nabla u^\varepsilon) = 0, \quad \text{in} \quad \Omega^{\varepsilon T}, \tag{2}$$

and for the reactive boundary condition, we have by the conservation of mass,

$$-\boldsymbol{\nu} \cdot \nabla u^\varepsilon = \partial_t v^\varepsilon \quad \text{on} \quad \Gamma^{\varepsilon T}. \tag{3}$$

For the crystal concentration, the rate of change is the net result of two opposing processes, precipitation and dissolution. This is given by

$$\partial_t v^\varepsilon = (r(u^\varepsilon) - w^\varepsilon) \quad \text{on} \quad \Gamma^{\varepsilon T}, \tag{4}$$

where $r(\cdot)$ is the precipitation rate while w denotes the rate of dissolution. We assume the following structure for the precipitation rate $r(u^\varepsilon)$

A1. $r : \Re \to [0, \infty)$ is locally Lipschitz .

A2. There exists a unique $u_* \geq 0$, such that
$$r(u^\varepsilon) = \left\{ \begin{array}{l} 0 \quad \text{for} \quad u^\varepsilon \leq u_*, \\ \text{strictly increasing for} \quad u^\varepsilon \geq u_* \quad \text{with} \quad r(\infty) = \infty. \end{array} \right.$$

All the equations are considered in dimensionless form. The diffusion constant has been scaled to 1, with the extension to positive definite tensor being straightforward. The dissolution process takes place only when the crystal precipitate is present (i.e. if $v(t, x) > 0$) and it is a surface process hence proceeds with a constant rate. We normalize this rate to 1. In

the absence of precipitate, the overall rate (precipitation minus dissolution) is either zero or positive depending upon the amount of solute present. Further, the absence of net gain in the crystal concentration under insufficient amount of solutes is related to the time-scale of observation. The derivation of the precipitation-dissolution is based on chemical kinetics and the ideas of solubility product for the crystals. For further discussions and derivation of this model, we refer to [16, 29]. A similar model leading to the dissolution fronts is given in [7].

To summarize the discussion above, the dissolution rate is

$$w \in H(v), \quad \text{where} \quad H(v) = \begin{cases} 0, & \text{if} \quad v < 0, \\ [0,1] & \text{if} \quad v = 0, \\ 1 & \text{if} \quad v > 0. \end{cases} \tag{5}$$

Remark 2.1 Since the precipitation rate r is monotonically increasing, under the setting above, a unique u^* exists for which $r(u^*) = 1$. If $u = u^*$ for all t and x, then the system is in equilibrium: no precipitation or dissolution occurs, since the precipitation rate is balanced by the dissolution rate regardless of the presence of absence of crystals.
The system (2)-(5) is complemented by the following initial and boundary conditions,

$$\begin{cases} u^\varepsilon(0,\cdot) &=& u_I, & \text{in} \quad \Omega^\varepsilon, \\ v^\varepsilon(0,\cdot) &=& v_I, & \text{on} \quad \Gamma^\varepsilon, \\ u^\varepsilon &=& 0 & \text{on} \quad \Gamma_D^T. \end{cases} \tag{6}$$

Note that (4) describes reaction of ions under both equilibrium and non-equilibrium conditions. The model (2) is a simplified setting for the model considered in [13, 15–17] and we refer to the cited literatures for more details.

We emphasize here the fact that no changes in the Ω^ε are encountered due to the dissolution or precipitation. In other words, the precipitate layer is very thin, so it does not change the boundary Γ^ε. An alternative situation, when Γ^ε and hence Ω^ε evolve in time depending on the solution is considered in [31, 32, 41, 43].

2.2 Weak formulation

Since the reaction term has a multi-valued description, we do not expect sufficient regularity for the existence of strong solutions except for in particular instances. To rectify this, we define appropriate weak solutions for the system of equations considered here. Let $(\cdot,\cdot)$ denote the L^2 inner product or duality pairing of H^1, H^{-1}. Also, we define $H_0^1(\Omega^\varepsilon)$ the space with $w \in H^1$ with homogeneous Dirichlet boundary condition on $\partial\Omega^\varepsilon \setminus \Gamma^\varepsilon$. The dual of $H_0^1(\Omega^\varepsilon)$ is the function space $H^{-1}(\Omega^\varepsilon)$. The definitions involving Ω insead of Ω^ε are similar.
We consider the following function spaces, where we follow the usual notations from functional analysis.

$$\begin{aligned} \mathcal{U}^\varepsilon &:= \{u \in L^2(0,T; H_0^1(\Omega^\varepsilon)) : \partial_t u \in L^2(0,T; H^{-1}(\Omega^\varepsilon))\}, \\ \mathcal{V}^\varepsilon &:= H^1(0,T; L^2(\Gamma_G^\varepsilon)), \\ \mathcal{W}^\varepsilon &:= \{w \in L^\infty(\Gamma^{\varepsilon T}) : 0 \le w \le 1\}. \end{aligned}$$

We assume that the initial conditions $(u_I, v_I) \in (H_0^1(\Omega^\varepsilon), H^1(\Gamma^\varepsilon))$. The definition of a weak solution is given as follows.

Definition 2.2 A triple $(u^\varepsilon, v^\varepsilon, w^\varepsilon) \in \mathcal{U}^\varepsilon \times \mathcal{V}^\varepsilon \times \mathcal{W}^\varepsilon$ is a weak solution of (2)-(6) if $u^\varepsilon(0,\cdot) = u_I, v^\varepsilon(0,\cdot) = v_I$ and

$$\begin{aligned} (\partial_t u^\varepsilon, \phi)_{\Omega^{\varepsilon T}} + (\nabla u^\varepsilon, \nabla\phi)_{\Omega^{\varepsilon T}} - (\mathbf{q}^\varepsilon u^\varepsilon, \nabla\phi)_{\Omega^{\varepsilon T}} &= -(\partial_t v^\varepsilon, \phi)_{\Gamma^{\varepsilon T}}, \\ (\partial_t v^\varepsilon, \theta)_{\Gamma^{\varepsilon T}} &= (r(u^\varepsilon) - w^\varepsilon, \theta)_{\Gamma^{\varepsilon T}}, \\ w^\varepsilon &\in H(v^\varepsilon) \quad \text{a.e. in} \quad \Gamma^{\varepsilon T}, \end{aligned} \tag{7}$$

for all $(\phi, \theta) \in L^2(0,T; H_0^1(\Omega^\varepsilon)) \times L^2(\Gamma^{\varepsilon T})$.

Remark 2.3 The existence of weak solutions of (2)-(6) has been proved in [17] by fixed point arguments, after regularizing the Heaviside function modelling the dissolution process. This yields a solution triple which converges to a solution to the original model when passing the regularization argument to zero. For the solutions $(u^\varepsilon, v^\varepsilon, w^\varepsilon)$ constructed in this way, the dissolution rate w^ε satisfies

$$w^\varepsilon = \begin{cases} 1 & \text{if} \quad v^\varepsilon > 0, \\ \min(r(u^\varepsilon), 1) & \text{if} \quad v^\varepsilon = 0, \\ 0 & \text{if} \quad v^\varepsilon < 0. \end{cases} \tag{8}$$

2.3 Known results

The existence and uniqueness results derived for the pore scale model in [13, 17, 44] remain valid in the present context. In [13, 17] the following is proved

Theorem 2.4 *Under assumptions (A.1) and (A.2), there exists a weak solution in the sense of Definition 2.2. In addition, the solution satisfies*

$$0 \leq u^\varepsilon, v^\varepsilon \leq M, \tag{9}$$

$$\|u^\varepsilon\|^2_{L^\infty(0,T;L^2(\Omega^\varepsilon))} + \|\nabla u^\varepsilon\|^2_{L^2(\Omega^{\varepsilon T})} + \|\partial_t u^\varepsilon\|^2_{L^2(0,T;H^{-1}(\Omega^\varepsilon))} + \|v^\varepsilon\|^2_{L^\infty(0,T;L^2(\Gamma^\varepsilon))} + \|\partial_t v^\varepsilon\|^2_{L^2(\Gamma^{\varepsilon T})} \leq C, \tag{10}$$

where M is a constant depending on the initial conditions, and $C > 0$ is a constant independent of $u^\varepsilon, v^\varepsilon, w^\varepsilon$ and ε.

We note that the estimates proved in [17] include an ε factor in front of the v^ε norms. This is due to the fact that the domain considered there is perforated (with periodicity ε), and the total measure of the boundaries where dissolution and precipitation may take place is of order ε^{-1}. Repeating the steps of the proof in the present case would lead to the estimate in Theorem 2.4.

The above estimates are not enough to guarantee uniqueness. In the wake of nonlinearities and discontinuities present in the reaction rate defined on a lower dimensional manifold, the L^2 stability with respect to initial data is out of reach. However, a L^1 contraction is achieved in [44], where the following result has been proven.

Theorem 2.5 *Assume (A.1) and (A.2) and consider two weak solutions $(u^{(i)\varepsilon}, v^{(i)\varepsilon}, w^{(i)\varepsilon}) \in \mathcal{U}^\varepsilon, \mathcal{V}^\varepsilon, \mathcal{W}^\varepsilon, i = 1, 2$ of (7) with initial values $(u_I^{(i)}, v_I^{(i)}, i = 1, 2)$ respectively. Then for any $t \in (0, T]$ we have*

$$\int_{\Omega^\varepsilon} |u^{(1)\varepsilon}(t,x) - u^{(2)\varepsilon}(t,x)|dx + \int_{\Gamma^\varepsilon} |v^{(1)\varepsilon}(t,x) - v^{(2)\varepsilon}(t,x)|dx \leq \int_{\Omega^\varepsilon} |u_I^{(1)}(x) - u_I^{(2)}(x)|dx + \int_{\Gamma^\varepsilon} |v_I^{(1)}(x) - v_I^{(2)}(x)|dx.$$

Note that Theorem 2.5 provides, in particular, the uniqueness of the solution.
The results above refer to the existence and uniqueness of a weak solution. For the numerical results we refer to [13], where the convergence of an Euler implicit discretization for the pore scale model (similar to the present one) is proved. For the core scale model, the convergence of the semi-discrete and of the fully discrete (conformal and mixed finite element) numerical schemes have been analyzed [33, 34].
The rigorous derivation of the macro scale model from the pore scale model in the classical homogenization context is carried out in [30]. Assuming the domain covered by a translation of a scaled unit cell with scaling parameter ε (see [1, 22–24, 38]), there homogenization techniques are employed to derive the upscaled (core scale) equations as the limit of $\varepsilon \searrow 0$. For the simpler geometry of a thin strip, the 1D upscaled model is rigorously justified in [17]. The situation here is in between, as the only oscillating part is the boundary of domain Ω^ε.

3 Upscaled equations

The flow equations are decoupled from the transport equation for ions. Hence, we can homogenize the velocity field separately. Here we assume that the velocity field $\mathbf{q}^\varepsilon$ is given, satisfies L^∞ bounds and a $\mathbf{q} \in L^\infty(\Omega) \cap H^1\Omega)$ exists s.t.

$$\|\mathbf{q}^\varepsilon - \mathbf{q}\|_{L^2(\Omega^T)} \searrow 0 \text{ as } \varepsilon \searrow 0. \tag{11}$$

For the specific case of Stokes equation, in [26–28] it is proved that the homogenized equation is the Stokes equation with Dirichlet boundary condition for the leading order term.

$$\begin{aligned} \nabla \cdot \mathbf{q} &= 0, && \text{in } \Omega, \\ \Delta \mathbf{q} &= \nabla P && \text{in } \Omega, \\ \mathbf{q} &= 0 && \text{on } \{y = 0\} \cup \{y = 1\}, \\ \mathbf{q} &= Qy(1-y)\mathbf{e}_1 && \text{on } \{x = 0\}. \end{aligned}$$

In fact, the cited references go beyond leading order terms. For the first order term, slip boundary conditions are derived. However, for our present purposes, the Dirichlet boundary condition suffices since for the concentration term we restrict

only to the leading order approximation. With the simple geometry Ω considered here, and under the parabolic inlet boundary conditions, we can solve the above equations exactly. It is straightforward to check that the unique solution of the above equations is

$$\mathbf{q} = Qy(1-y)\mathbf{e}_1.$$

The interesting aspect here is the derivation of the upscaled equation for the reaction terms. Indeed, the main result of this chapter is the derivation of the following result. The homogenized variables u, v, w satisfy the following system of equations.

$$\partial_t u - \Delta u + \mathbf{q}\nabla u = 0 \qquad \text{in } \Omega^{)}, \tag{12}$$

$$-\boldsymbol{\nu}\cdot\nabla u = \int_\Gamma \partial_t v ds \quad \text{on } (0,T]\times(0,1), \tag{13}$$

$$\partial_t v = r(u) - w \quad \text{on } (0,1)\times\Gamma^T, \tag{14}$$

$$w \in H(v). \tag{15}$$

Note that the above equations are defined in domains where the boundaries are flat. Further, the information about the geometry of the rough boundary Γ^ε in the original domain is incorporated through terms defined on $\Gamma-$ which is scaled from a unit period of Γ^ε. Performing computations on domains with flat boundaries is much cheaper compared to smaller mesh sizes required for resolving the oscillations at Γ^ε. This is the essential advantage of this upscaling.

The results are further consistent with intuitive arguments. Replacing the rough boundary by a flat one in a physically consistent manner requires correcting the flux. The above upscaling result show that in each point of the flat boundary, the normal flux (in fact its leading order approximation) is obtained by simply accounting for the flux over the entire length of one period of the rough boundary associated with that point.

The goal of this paper is proving the convergence of the upscaling procedure. We start by defining the concept for solution for (12)-(15).

Definition 3.1 A triple $(u,v,w) \in L^2(0,T;H_0^1(\Omega)) \times L^2(0,T;L^2((0,1)\times\Gamma)) \times L^\infty((0,T)\times(0,1)\times\Gamma)$ is a weak solution of (12)-(15) if $u(0,\cdot) = u_I, v(0,\cdot) = v_I$ and

$$\begin{aligned} -(u,\partial_t\phi)_{\Omega^T} + (\nabla u,\nabla\phi)_{\Omega^T} - (\mathbf{q}u,\nabla\phi)_{\Omega^T} + (\partial_t v,\phi)_{(0,T]\times(0,1)\times\Gamma} &= (u_I,\phi(0,x))_\Omega, \\ (\partial_t v,\theta)_{(0,T]\times(0,1)\times\Gamma} - (r(u)-w,\theta)_{(0,T]\times(0,1)\times\Gamma} &= 0, \\ w &\in H(v) \quad \text{a.e.}, \end{aligned}$$

for all $\phi \in H^1(\Omega^T), \phi(T,x) = 0; \phi = 0$ on Γ_D and $\theta \in L^2(0,T;L^2((0,1)\times\Gamma))$.

The main result of this paper is:

Theorem 3.2 *Along any sequence $\varepsilon \searrow 0$, the solution triple $(u^\varepsilon, v^\varepsilon, w^\varepsilon)$ in the sense of Definition 2.2 converges to (u,v,w), the solution introduced in Definition 3.1.*

In what follows, we prove the above Theorem 3.2. We have taken a restricted class of test function for ϕ (compare this with ϕ in Definition 2.2) which helps in dealing with the low regularity of $\partial_t u^\varepsilon$. The estimates for Ω^ε are easily carried over to the estimates for Ω and the trace theorem also provides a compactness for the traces defined at the boundary Γ^ε. However, Γ^ε depends on ε and therefore the estimates are defined in a $\varepsilon-$dependent domain. We use the unfolding operator to map the estimates and integrals from $\varepsilon-$dependent domains to a fixed domain. Also, the non-linearities need strong convergence for which we use translation estimates. Further, we connect the limits from the unfolded sequence defined at the boundary to the limits obtained from the estimates in Ω.

4 A priori estimates

In this section, we begin with estimate dealing with translation in time. Next, we deal with the periodic unfolding operator defined for the boundaries. This is followed by the a priori estimates both for the domain and the boundary. Let us begin with the following lemma.

Lemma 4.1 *Let $\eta > 0$ and $(u^\varepsilon, v^\varepsilon, w^\varepsilon)$ be a weak solution of (7) in the sense of Definition 2.2. Then the following estimate is uniform in η,*

$$\int_0^{T-\eta}\int_{\Omega^\varepsilon} |u^\varepsilon(t+\eta,x) - u^\varepsilon(t,x)|^2 dxdt \le C\eta. \tag{16}$$

P r o o f. From $(7)_1$ and its time shifted (t becoming $t+\eta$) variant, assuming $\phi = 0$ whenever $t > T - \eta$ one gets

$$\int_0^{T-\eta} (\partial_t(u^\varepsilon(t+\eta,x) - u^\varepsilon(t,x)), \phi)\, dt + \int_0^{T-\eta}\int_{\Omega^\varepsilon} (\nabla u^\varepsilon(t+\eta,x) - \nabla u^\varepsilon(t,x))\nabla\phi dxdt$$
$$- \int_0^{T-\eta}\int_{\Omega^\varepsilon} \mathbf{q}^\varepsilon(u^\varepsilon(t+\eta,x) - u^\varepsilon(t,x))\nabla\phi dxdt = -\int_0^{T-\eta}\int_{\Gamma^\varepsilon} \partial_t(v^\varepsilon(t+\eta,x) - v^\varepsilon(t,x))\phi dxdt.$$

Choosing $\phi(t,x) = \int_t^{t+\eta} u^\varepsilon(s,x)ds \in H^1(0,T;H_0^1(\Omega^\varepsilon))$ gives

$$\int_0^{T-\eta}\int_{\Omega^\varepsilon} |u^\varepsilon(t+\eta,x) - u^\varepsilon(t,x)|^2 dxdt = -\int_{\Omega^\varepsilon} (u^\varepsilon(\eta,x) - u^\varepsilon(0,x)) \left(\int_0^\eta u^\varepsilon(s,x)ds\right) dx$$
$$+ \int_{\Omega^\varepsilon} (u^\varepsilon(T,x) - u^\varepsilon(T-\eta,x)) \left(\int_{T-\eta}^T u^\varepsilon(s,x)ds\right) dx + \int_{\Omega^\varepsilon} \left|\int_{T-\eta}^T \nabla u^\varepsilon(s,x)ds\right|^2 dxdt$$
$$- \int_{\Omega^\varepsilon} \left|\int_0^\eta \nabla u^\varepsilon(s,x)ds\right|^2 dxdt - \int_0^{T-\eta}\int_{\Omega^\varepsilon} \mathbf{q}^\varepsilon(u^\varepsilon(t+\eta,x) - u^\varepsilon(t,x)) \left(\nabla \int_t^{t+\eta} u^\varepsilon(s,x)ds\right) dxdt$$
$$+ \int_0^{T-\eta}\int_{\Gamma^\varepsilon} \partial_t(v^\varepsilon(t+\eta,x) - v^\varepsilon(t,x)) \left(\int_t^{t+\eta} u^\varepsilon(s,x)ds\right) dxdt.$$

We treat each term on the right, denoted by $\mathcal{I}_i, i = 1,\dots,6$, separately. The L^∞ estimate for u^ε gives for both $\mathcal{I}_1$ and $\mathcal{I}_2$

$$|\mathcal{I}_1| \le C\eta, \qquad |\mathcal{I}_2| \le C\eta.$$

For $\mathcal{I}_3$, we use Cauchy Schwarz and the estimates on the gradient in Theorem 2.4 to obtain

$$|\mathcal{I}_3| \le C\eta.$$

Because of its sign, $\mathcal{I}_4$ needs no further estimate. Next, by L^∞ estimates for $u^\varepsilon, \mathbf{q}^\varepsilon$ and the gradient estimates in Theorem 2.4, for $\mathcal{I}_5$ one obtains

$$\begin{aligned} |\mathcal{I}_5| &\le C\int_0^{T-\eta} \|u^\varepsilon(t+\eta) - u^\varepsilon(t)\|_{L^2(\Omega^\varepsilon)} \left\|\int_t^{t+\eta} \nabla u^\varepsilon(s)ds\right\| dt \\ &\le \frac{1}{2}\int_0^{T-\eta} \|u^\varepsilon(t+\eta,x) - u^\varepsilon(t,x)\|_{L^2(\Omega^\varepsilon)} + C\eta. \end{aligned}$$

Furthermore, by triangle inequality and the $L^2(0,T;L^2(\Gamma^\varepsilon))$ estimates of $\partial_t v^\varepsilon$, we have

$$|\mathcal{I}_6| \le C\|\partial_t v^\varepsilon\|_{L^2(\Gamma^{\varepsilon T})}\eta \le C\eta$$

where we have again used the L^∞ estimate for u^ε. Collecting the above computations leads to the assertion. □

4.1 The boundary unfolding operator

We start with introducing the unfolding operator and describe some of its properties. For more details for the properties and the proofs, we refer to [11] for unfolding operators in general, and to [12] for the boundary unfolding operator.

Following [12], we define the boundary unfolding operator as:

Definition 4.2 Let $\phi^\varepsilon : (0,1)\times\Gamma \mapsto \Gamma^\varepsilon$ be defined as $(x,(z,h(z))) \mapsto \left(\varepsilon\left\lfloor\frac{x}{\varepsilon}\right\rfloor + \varepsilon z, \varepsilon h(z)\right)$. The unfolding operator T^ε maps a function $u : \Gamma^\varepsilon \to \Re$ to the function $u\circ\phi^\varepsilon : (0,1)\times\Gamma \to \Re$.

Note that the unfolding operator is defined here only for the boundary and not for the whole domain. For the unfolding operator defined in the fully periodic context (classical homogenization), we refer to [8, 11] and to [36] for an application of this technique relevant to the present context . Below, we list some simple but useful propositions.

Proposition 4.3 *T^ε is linear.*

Proposition 4.4 *Let u,v be functions $\Gamma^\varepsilon \to \Re$. Then $T^\varepsilon(uv) = T^\varepsilon u T^\varepsilon v$.*

The proofs for Proposition 4.3 and Proposition 4.4 are straightforward and therefore omitted.

Proposition 4.5 *For $u \in L^1(\Gamma^\varepsilon)$, it holds that*

$$\int\limits_{(0,1)\times\Gamma} T^\varepsilon u(x,(z,h(z)))dxds = \int\limits_{\Gamma^\varepsilon} u(x)\,dx.$$

P r o o f. Using the periodicity of h, a straightforward computation provides :

$$\begin{aligned}\int\limits_{(0,1)\times\Gamma} T^\varepsilon u(x,z,h(z))dxds &= \int\limits_{(0,1)\times\Gamma} u\left(\varepsilon\left(\left\lfloor\frac{x}{\varepsilon}\right\rfloor + z\right), \varepsilon h(z)\right)dxds \\ &= \varepsilon\sum_{k=0}^{\frac{1}{\varepsilon}-1}\int\limits_{\Gamma} u\left(\varepsilon k + \varepsilon z, \varepsilon h(z)\right)ds \\ &= \sum_{k=0}^{\frac{1}{\varepsilon}-1}\int\limits_{k\varepsilon}^{(k+1)\varepsilon} u\left(x, \varepsilon h\left(\frac{x}{\varepsilon}\right)\right)ds = \int\limits_{\Gamma^\varepsilon} u ds^\varepsilon,\end{aligned}$$

where ds is the differential along the curve Γ and ds^ε the differential along Γ^ε. □

Based on the above result, we obtain the following:

Proposition 4.6 *Let $u \in L^2(\Gamma^\varepsilon)$. Then $T^\varepsilon u \in L^2((0,1)\times\Gamma)$ and T^ε is a linear isometry between $L^2(\Gamma^\varepsilon)$ and $L^2((0,1)\times\Gamma)$.*

P r o o f. Suppose that $u \in L^2(\Gamma^\varepsilon)$. Then $|u|^2 \in L^1(\Gamma^\varepsilon)$. Using propositions 4.4 and 4.5 we find

$$\int\limits_{(0,1)\times\Gamma} |T^\varepsilon u|^2\,dx = \int\limits_{(0,1)\times\Gamma} T^\varepsilon |u|^2\,dx = \int\limits_{\Gamma^\varepsilon} |u|^2 dx < \infty.$$

Also $\|T^\varepsilon u\|_{L^2((0,1)\times\Gamma)} = \|u\|_{L^2(\Gamma^\varepsilon)}$ and together with Proposition 4.3, this implies that T^ε is a linear isometry between $L^2(\Gamma^\varepsilon)$ and $L^2((0,1)\times\Gamma)$. □

The above linear isometry is an important result as it provides a way to connect the unfolded sequence defined on a fixed domain with the original variables defined on an $\varepsilon-$dependent domain. This makes it possible to use the estimates obtained for Γ^ε for the unfolded sequence directly.

4.2 Estimates in the domain Ω

In this section we refer to the solution triple introduced in Definition 2.2 and proceed with the a priori estimates in both Ω and Γ^ε. Since $\Omega \subset \Omega^\varepsilon$, the estimate gets carried over and we obtain the following estimate from Theorem 2.4:

$$\|\nabla u^\varepsilon\|^2_{L^2(0,T;L^2(\Omega))} + \|\partial_t v^\varepsilon\|^2_{L^2(0,T;L^2(\Gamma^\varepsilon))} + \|v^\varepsilon\|^2_{L^2(0,T;L^2(\Gamma^\varepsilon))} \le C. \tag{17}$$

The above estimate is valid in fact for the restriction of u^ε to Ω, which is also further denoted by u^ε to simplify the writing. We have:

Lemma 4.7 *Let u^ε be the first component of the solution triple in Definition 2.2. A $u_0 \in L^2(o,T;H^1_0(\Omega))$ exists s.t. along a sequence $\varepsilon \searrow 0$,*

$$\nabla u^\varepsilon \rightharpoonup \nabla u_0 \text{ weakly in } L^2(0,T;\Omega). \tag{18}$$

$$u^\varepsilon \to u_0 \text{ strongly in } L^2(0,T;\partial\Omega). \tag{19}$$

P r o o f. The first part of the lemma follows from the uniform bounds of ∇u^ε as in (17). To prove (19), we note that $\partial_t u^\varepsilon \in L^2(0,T;H^*(\Omega))$ where H^* is the dual of $H^1_{0,\partial\Omega}(\Omega)$ with $H^1_{0,\partial\Omega}(\Omega)$ referring to the space of H^1 functions with homogeneous Dirichlet boundary conditions on $\partial\Omega$. Note the difference with previously introduced $H^1_0(\Omega^\varepsilon)$ or $H^1_0(\Omega)$ where homogeneous Dirichlet boundary conditions are taken only on $\partial\Omega^\varepsilon \setminus \Gamma^\varepsilon$ respectively $\partial\Omega \setminus \Gamma$. With $u^\varepsilon \in L^2(0,T;H^1_0(\Omega))$ and $\partial_t u^\varepsilon \in L^2(0,T;H^*(\Omega))$, we conclude that u^ε converges strongly in $L^2(0,T;L^2(\Omega))$.
Now consider the integral $\mathcal{I}^\varepsilon$

$$\mathcal{I}^\varepsilon := \int_0^T \|u^\varepsilon(t) - u_0(t)\|^2_{L^2(\partial\Omega)} dt. \tag{20}$$

Following the proof of the trace theorem (see [18], chapter 5.5), we have

$$\mathcal{I}^\varepsilon \leq \int_0^T C\|u^\varepsilon - u_0\|_{L^2(\Omega)} \left(\|u^\varepsilon - u_0\|_{L^2(\Omega)} + \|\nabla(u^\varepsilon - u_0)\|_{L^2(\Omega)}\right) dt.$$

Using Cauchy Schwarz, the bounds on the gradients, and the semi-continuity of the norms, we obtain

$$\mathcal{I}^\varepsilon \leq C\|u^\varepsilon - u_0\|_{L^2(\Omega^T)}$$

from which the assertion follows. □

The original equations are defined in Ω^ε and by construction also in Ω as $\Omega \subset \Omega^\varepsilon$. We now prove that the contributions for the integrals in $\Omega^\varepsilon \setminus \Omega$ are negligible as $\varepsilon \searrow 0$. We achieve this by decomposing the integrals defined on Ω^ε. Note that by decomposing the integrals in domains Ω and $\Omega^\varepsilon \setminus \Omega$ we have the property that the measure of $\Omega^\varepsilon \setminus \Omega$ becomes negligible as $\varepsilon \to 0$. Also, the test functions are defined independent of ε, which we will use here. We start with the following direct consequence of the dominated convergence theorem.

Proposition 4.8 *For any function $f \in L^1(\Omega)$, with $E \subset \Omega$, it holds that $\int_E |f| \searrow 0$ as $meas(E) \searrow 0$.*

The following lemma shows that the contributions of the integrals on the set $\Omega^\varepsilon \setminus \Omega$ are negligible.

Lemma 4.9 *For any $\phi \in H^1(\Omega^T)$ it holds*

$$\lim_{\varepsilon \searrow 0} \left\{ \int_0^T \int_{\Omega^\varepsilon \setminus \Omega} (-u^\varepsilon \partial_t \phi + \nabla u^\varepsilon \nabla \phi + \boldsymbol{q}^\varepsilon u^\varepsilon \nabla \phi)\, dx dt \right\} = 0 \tag{21}$$

P r o o f. Let us denote the integrals in (21) by $\mathcal{I}_i,\ i = 1,2,3$ respectively. For $\mathcal{I}_1$ one has

$$\begin{aligned} |\mathcal{I}_1| &\leq \|u^\varepsilon\|_{L^2(0,T;L^2(\Omega^\varepsilon \setminus \Omega))} \|\partial_t \phi\|_{L^2(0,T;L^2(\Omega^\varepsilon \setminus \Omega)} \\ &\leq \|u^\varepsilon\|_{L^2(0,T;L^2(\Omega^\varepsilon))} \|\partial_t \phi\|_{L^2(0,T;L^2(\Omega^\varepsilon \setminus \Omega)} \leq C\|\partial_t \phi\|_{L^2(0,T;L^2(\Omega^\varepsilon \setminus \Omega)}. \end{aligned}$$

Since $\partial_t \phi \in L^2(0,T;L^2(\Omega^\varepsilon))$ by Proposition 4.8 we conclude that $\mathcal{I}_1 \searrow 0$ as $\varepsilon \searrow 0$.
The estimates for the other integrals are similar. □

4.3 The boundary estimates

By Theorem 2.4 for v^ε and w^ε one has:

$$\|v^\varepsilon\|^2_{L^\infty(0,T;L^2(\Gamma^\varepsilon))} + \|\partial_t v^\varepsilon\|^2_{L^2(\Gamma^{\varepsilon T})} + \|w^\varepsilon\|^2_{L^2(\Gamma^{\varepsilon T})} \leq C.$$

The unfolding operator defined at the boundary maps these estimates to a domain that does not depend on ε. In terms of the unfolded sequence and using the L^2 isometry, the estimate above become

$$\|T^\varepsilon v^\varepsilon\|^2_{L^\infty(0,T;L^2((0,1)\times\Gamma))} + \|\partial_t T^\varepsilon v^\varepsilon\|^2_{L^2((0,1)\times\Gamma\times(0,T))} + \|T^\varepsilon w^\varepsilon\|^2_{L^2((0,1)\times\Gamma\times(0,T)} \leq C. \tag{22}$$

The bounds above immediately imply the following convergence result:

Lemma 4.10 *There exists* $(u, v, w) \in L^2(0,T; L^2((0,1)\times\Gamma))$ *such that* $\partial_t v \in L^2(0,T; L^2((0,1)\times\Gamma))$ *and along a sequence* $\varepsilon \searrow 0$ *it holds*

$$\begin{aligned} T^\varepsilon v^\varepsilon &\rightharpoonup v \text{ weakly in } L^2(0,T; L^2((0,1)\times\Gamma)) \\ T^\varepsilon w^\varepsilon &\rightharpoonup w \text{ weakly in } L^2(0,T; L^2((0,1)\times\Gamma)) \\ T^\varepsilon u^\varepsilon &\rightharpoonup u \text{ weakly in } L^2(0,T; L^2((0,1)\times\Gamma)) \\ T^\varepsilon \partial_t v^\varepsilon &\rightharpoonup \partial_t v \text{ weakly in } L^2(0,T; L^2((0,1)\times\Gamma)). \end{aligned}$$

Note that both the unfolded triples $(T^\varepsilon u^\varepsilon, T^\varepsilon v^\varepsilon)$ and their limit are defined on $(0,T]\times(0,1)\times\Gamma$. Also Note that the convergence for $T^\varepsilon v^\varepsilon$ and $T^\varepsilon u^\varepsilon$ is weak, which is not sufficient for passing to the limit in the non-linear terms. We therefore need to improve the convergence. We start with the following:

Proposition 4.11 *For the first component in the solution triple* $(u^\varepsilon, v^\varepsilon, w^\varepsilon)$ *the following holds uniformly in* ε*:*

$$\|u^\varepsilon\|^2_{L^2(0,T;H^{\frac{1}{2}}(\Gamma^\varepsilon))} \leq C. \tag{23}$$

P r o o f. In view of $(6)_3$, the Poincaré inequality and the trace estimate give

$$\|u^\varepsilon\|^2_{L^2(0,T;H^{\frac{1}{2}}(\Gamma^\varepsilon))} \leq C\|\nabla u^\varepsilon\|^2_{L^2(0,T;L^2(\Omega^\varepsilon))}.$$

Also, it is to be noted that the boundary is uniformly Lipschitz continuous, as

$$|h^\varepsilon(x) - h^\varepsilon(y)| \leq \varepsilon|h(\frac{x}{\varepsilon}) - h(\frac{y}{\varepsilon})| \leq L_h|x-y|,$$

where L_h is the Lipschitz constant of h. Further, note that C is independent of ε (see [6] for a discussion on this issue and also [35] P.121). Combining this with the estimates in Theorem 2.4 gives the assertion. □

The strong convergence for $T^\varepsilon u^\varepsilon$ and $T^\varepsilon v^\varepsilon$ will be proved based on translation estimates. To achieve this the translation along the (rough) boundary needs to be defined properly. We therefore let I_C be a bounded interval in $\Re$ and $h_C : I_C \mapsto \Re$ be a Lipschitz function. Consider $\widetilde{h}_C : \Re \mapsto \Re$ a Lipschitz continuous extension of h_C such that $\widetilde{h}_C$ has compact support. Based on these we define the curves Γ_C and $\widetilde{\Gamma}_C$

$$\begin{aligned} \Gamma_C &:= \{(z, h_C(z)) \mid z \in I_C\}, \\ \widetilde{\Gamma}_C &:= \{(z, \widetilde{h}_C(z)) \mid z \in \Re\}. \end{aligned}$$

The above setting facilitates in defining the smooth extension $\widetilde{f} : \widetilde{\Gamma}_C \mapsto \Re$ for any given function $f : \Gamma_C \mapsto \Re$, $f \in H^{\frac{1}{2}}(\Gamma_C)$. Assume now that the extension $\widetilde{f}$ has compact support. Next, let $\bar{f} : \Re \mapsto \Re$ be defined as

$$\bar{f}(z) := \widetilde{f}(z, \widetilde{h}_C(z)).$$

Now for any given real number $\eta > 0$, we define the translation

$$\triangle_\eta \bar{f}(\cdot) := \bar{f}(\cdot + \eta) - \bar{f}(\cdot).$$

By an abuse of notation, $\triangle_\eta f$ will be often used in the above sense.

Having introduced the translation we now estimate the translation for a given function $f \in H^{\frac{1}{2}}(\Gamma_C)$:

Lemma 4.12 *Given* $f \in H^{\frac{1}{2}}(\Gamma_C)$ *the following translation estimate holds*

$$\|\triangle_\eta f\|_{L^2(\widetilde{\Gamma}_C)} \leq C|\eta|^{\frac{1}{2}}.$$

P r o o f. The proof is straightforward in the Fourier space. Let $\widetilde{f}$ be the extension of f as above with compact support. For any $f \in H^{\frac{1}{2}}(\Gamma_C)$ we have

$$\|f\|_{H^{\frac{1}{2}}(\widetilde{\Gamma}_C)} \leq C\|\widetilde{f}\|_{H^{\frac{1}{2}}(\Re)} \leq C.$$

Let $\hat{f}$ denote the Fourier transform of $\widetilde{f}$. For the $H^{\frac{1}{2}}(\Re)$ semi-norm, we have the following equivalent characterization in Fourier space

$$\|\widetilde{f}\|_{H^{\frac{1}{2}}(\Re)} = \int_{\Re} |\omega||\hat{f}|^2 d\omega < C, \tag{24}$$

for any $\widetilde{f} \in H^{\frac{1}{2}}(\Re)$ with its $H^{\frac{1}{2}}$ norm uniformly bounded. Using the L^2 isometry of the Fourier transform

$$\int_{\widetilde{\Gamma}_C} \left|\triangle_\eta f\right|^2 ds \leq C \int_{\Re} \left|\triangle_\eta \widetilde{f}\right|^2 dx = C \int_{\Re} \left|(1-e^{i\omega\eta})^2 \hat{f}(\omega)\right|^2 d\omega.$$

The right hand side can be re-written as

$$\int_{\Re} (1-e^{i\omega h})^2 |\hat{f}(\omega)|^2 d\omega = \int_{\Re} \frac{(1-e^{i\omega\eta})^2}{|\eta\omega|} |\eta\omega||\hat{f}(\omega)|^2 d\omega \leq C|\eta| \int_{\Re} |\omega||\hat{f}(\omega)|^2 d\omega \tag{25}$$

and as noted above, the last term on the right hand side is bounded because $\widetilde{f} \in H^{\frac{1}{2}}(\Re)$. It is straightforward to check that

$$\frac{(1-e^{i\omega\eta})^2}{|\omega\eta|} \leq C.$$

This leads to

$$\int_{\widetilde{\Gamma}_C} \left|\triangle_\eta f\right|^2 ds \leq C|\eta| \tag{26}$$

where C depends on the $H^{\frac{1}{2}}$ norm. □

Before using the translation estimate, we prove the following.

Proposition 4.13 *Given $u^\varepsilon : \Gamma^\varepsilon \mapsto \Re$, the translation with respect to x commutes with the unfolding operator:*

$$\triangle_{\eta_x}(T^\varepsilon u^\varepsilon)(x,(z,h(z))) = T^\varepsilon(\triangle_{\eta_x} u^\varepsilon)(x,(z,h(z))). \tag{27}$$

P r o o f. Note that,

$$\begin{aligned} \triangle_{\eta_x} T^\varepsilon u^\varepsilon &:= T^\varepsilon u^\varepsilon(x+\eta_x,(z,h(z))) - T^\varepsilon u^\varepsilon(x,(z,h(z))) && (28)\\ &= u^\varepsilon\left(\varepsilon\left\lfloor\frac{x}{\varepsilon}\right\rfloor + k\varepsilon + \varepsilon z, \varepsilon h(z)\right) - u^\varepsilon\left(\varepsilon\left\lfloor\frac{x}{\varepsilon}\right\rfloor + \varepsilon z, \varepsilon h(z)\right) \quad \text{(by definition)} && (29)\end{aligned}$$

where $k = \lfloor\frac{\eta_x+x}{\varepsilon}\rfloor - \lfloor\frac{x}{\varepsilon}\rfloor$. For the right hand side,

$$\begin{aligned} T^\varepsilon \triangle_{\eta_x} u^\varepsilon &= T^\varepsilon\left(u^\varepsilon(x+\eta_x, h^\varepsilon(x+\eta_x)) - u^\varepsilon(x,h^\varepsilon(x))\right)\\ &= T^\varepsilon u^\varepsilon(x+\eta_x,h^\varepsilon(x+\eta_x)) - T^\varepsilon u^\varepsilon(x,h^\varepsilon(x))\\ &= u^\varepsilon\left(\varepsilon\left\lfloor\frac{x+\eta_x}{\varepsilon}\right\rfloor + \varepsilon z, \varepsilon h(z)\right) - u^\varepsilon\left(\varepsilon\left\lfloor\frac{x}{\varepsilon}\right\rfloor + \varepsilon z, \varepsilon h(z)\right)\\ &= u^\varepsilon\left(\varepsilon\left\lfloor\frac{x}{\varepsilon}\right\rfloor + k\varepsilon + \varepsilon z, \varepsilon h(z)\right) - u^\varepsilon\left(\varepsilon\left\lfloor\frac{x}{\varepsilon}\right\rfloor + \varepsilon z, \varepsilon h(z)\right). \end{aligned}$$

Using (29) proves the proposition. □

Proposition 4.13 gives the estimate

$$\|\triangle_{\eta_x} T^\varepsilon u^\varepsilon\|_{L^2((0,T)\times(0,1)\times\Gamma)} = \|T^\varepsilon(\triangle_{\eta_x} u^\varepsilon)\|_{L^2((0,T)\times(0,1)\times\Gamma)} = \|\triangle_{\eta_x} u^\varepsilon\|_{L^2(\Gamma^\varepsilon T)}, \tag{30}$$

which is used to obtain the strong convergence result.

For the remaining part of the section, by "convergence" we mean in fact the convergence along a sequence $\varepsilon \searrow 0$. Moreover, when referring to a pair or a triple, the sequence $\varepsilon \searrow 0$ should be understood as the convergent subsequence of the previously convergent (sub)sequence.

Lemma 4.14 *With $u \in L^2((0,T)\times(0,1)\times\Gamma)$ being the weak limit in Lemma 4.10,*

$$T^\varepsilon u^\varepsilon \to u \text{ strongly in } L^2\left((0,T)\times(0,1)\times\Gamma\right).$$

Proof. For a.e. $t \in (0,T)$,

$$\begin{aligned} \triangle_{\eta_z} T^\varepsilon u^\varepsilon &= T^\varepsilon u^\varepsilon(x,(z+\eta_z,h(z+\eta_z))) - T^\varepsilon u^\varepsilon(x,(z,h(z))) \\ &= u^\varepsilon(\varepsilon\lfloor\tfrac{x}{\varepsilon}\rfloor + \varepsilon z + \varepsilon\eta_z, \varepsilon h(z+\eta_z)) - u^\varepsilon(\varepsilon\lfloor\tfrac{x}{\varepsilon}\rfloor + \varepsilon z, \varepsilon h(z)) \end{aligned} \tag{31}$$

in terms of translation for u^ε. Denote the right hand side by $\mathcal{I}_{\eta_z}$. Note that this is nothing but a translation along the curve Γ and hence, we can use Lemma 4.12 to obtain

$$\|\mathcal{I}_{\eta_z}\|_{L^2((0,T)\times(0,1)\times\Gamma} \leq C|\eta_z|^{\frac{1}{2}}.$$

Next, we consider the translation along x. We note that

$$\|\triangle_{\eta_x} T^\varepsilon u^\varepsilon\| = \|\triangle_{\eta_x} T^\varepsilon u^\varepsilon\| = \|\triangle_{\eta_x} u^\varepsilon\|_{L^2(\Gamma^\varepsilon)}.$$

We use (30) together with the Lemma 4.12 to obtain

$$\|\triangle_{\eta_x} u^\varepsilon\|_{L^2(\Gamma^{\varepsilon T})} \leq C|\eta_x|^{\frac{1}{2}}.$$

Hence, we have the translations in x and z directions controlled which implies

$$(\|\triangle_{\eta_x}\|, \|\triangle_{\eta_z}\|) \searrow (0,0), \text{ along a sequence } (|\eta_x|,|\eta_z|) \searrow (0,0).$$

For the strong convergence, the time translations have to be dealt with. With $\eta_t \in (0,T)$, the L^2-isometry of the boundary unfolding operator gives

$$\begin{aligned} &\int_0^{T-\eta_t} \int_{\Gamma\times(0,1)} |T^\varepsilon u^\varepsilon(t+\eta_t,x,(z,h(z))) - T^\varepsilon u^\varepsilon(t,x,(z,h(z)))|^2 \, ds dx dt \\ &\qquad = \int_0^{T-\eta_t} \int_{\Gamma^\varepsilon} |u^\varepsilon(t+\eta_t,x) - u^\varepsilon(t,x)|^2 \, dx dt. \end{aligned}$$

Denote the left side by $\mathcal{I}$ and the translation operator by $\triangle_{\eta_t}$. As before, the trace theorem gives

$$\mathcal{I} \leq C \int_0^{T-\eta_t} \|\triangle_{\eta_t} u^\varepsilon(t,\cdot)\|_{L^2(\Omega^\varepsilon)} \left(\|\triangle_{\eta_t} u^\varepsilon(t,\cdot)\|_{L^2(\Omega^\varepsilon)} + \|\triangle_{\eta_t}(\nabla u^\varepsilon(t,\cdot))\|_{L^2(\Omega^\varepsilon)} \right) dt,$$

where the right side can be estimated by using Cauchy Schwarz inequality

$$\mathcal{I} \leq C \left(\int_0^{T-\eta_t} \|\triangle_{\eta_t} u^\varepsilon(t,\cdot)\|^2_{L^2(\Omega^\varepsilon)} dt \right)^{\frac{1}{2}} \left(\int_0^{T-\eta_t} \|\triangle_{\eta_t}(\nabla u^\varepsilon(t,\cdot))\|^2_{L^2(\Omega^\varepsilon)} dt \right)^{\frac{1}{2}} + C \int_0^{T-\eta_t} \|\triangle_{\eta_t} u^\varepsilon(t,\cdot)\|^2_{L^2(\Omega^\varepsilon)} dt.$$

Using the $L^2(0,T;L^2(\Omega^\varepsilon))$ bounds on the gradient, the above inequality reduces to

$$\mathcal{I} \leq C \left(\int_0^{T-\eta_t} \|\triangle_{\eta_t} u^\varepsilon(t,\cdot)\|^2_{L^2(\Omega^\varepsilon)} dt \right)^{\frac{1}{2}} + C \int_0^{T-\eta_t} \|\triangle_{\eta_t} u^\varepsilon(t,\cdot)\|^2_{L^2(\Omega^\varepsilon)} dt.$$

Now we use Lemma 4.1 to obtain

$$\mathcal{I} \leq C \left(\eta_t^{\frac{1}{4}} + \eta_t^{\frac{1}{2}} \right)$$

and with $\eta_t \searrow 0$, we conclude that the translations in time are controlled.

By Riesz-Kolmogorov compactness criterion, we conclude that $T^\varepsilon u^\varepsilon$ converges strongly in $L^2((0,T)\times(0,1)\times\Gamma)$. □

With the strong convergence of $T^\varepsilon u^\varepsilon$ established, we proceed to treat the non-linear terms on the boundary.

Lemma 4.15 *It holds*

$$T^\varepsilon r\left(u^\varepsilon\right) \to r(u) \text{ strongly in } L^2\left((0,T)\times(0,1)\times\Gamma\right).$$

P r o o f. Since r is Lipschitz, Proposition 4.6 gives

$$\|T^\varepsilon r\left(u^\varepsilon\right)\|^2_{L^2((0,T)\times(0,1)\times\Gamma)} = \|r\left(u^\varepsilon\right)\|^2_{L^2(\Gamma^{\varepsilon T})} \le C\|u^\varepsilon\|^2_{L^2(\Gamma^{\varepsilon T})} \le C,$$

showing that the sequence $T^\varepsilon r\left(u^\varepsilon\right)$ is bounded uniformly (w.r.t. ε) in L^2 sense. Further, by Lemma 4.14, as $\varepsilon \searrow 0$

$$\|T^\varepsilon r\left(u^\varepsilon\right) - r(u)\| = \|r\left(T^\varepsilon u^\varepsilon\right) - r(u)\| \le L_r\|T^\varepsilon u^\varepsilon - u\| \to 0,$$

where the norms are in $L^2((0,T)\times(0,1)\times\Gamma)$. □

Next, we improve the convergence of $T^\varepsilon v^\varepsilon$; the convergence

Lemma 4.16 *With v in Lemma 4.10,*

$$T^\varepsilon v^\varepsilon \to v \text{ strongly in } L^2\left((0,T)\times(0,1)\times\Gamma\right).$$

P r o o f. The idea is again based on translation. First, we note that $w^\varepsilon \in H(v^\varepsilon)$ satisfies

$$w^\varepsilon = \begin{cases} 1 & \text{if} \quad v^\varepsilon > 0, \\ \min(r(u^\varepsilon), 1) & \text{if} \quad v^\varepsilon = 0, \\ 0 & \text{if} \quad v^\varepsilon < 0. \end{cases}$$

and with this we conclude that w^ε is monotonically increasing with respect to v^ε. We re-write the equation $(7)_2$ by a change of co-ordinates,

$$\partial_t T^\varepsilon v^\varepsilon = T^\varepsilon r(u^\varepsilon) - T^\varepsilon w^\varepsilon \text{ in the sense of distributions.}$$

Our approach is close to that used in [39]. Since, $\partial_t v^\varepsilon$ is in L^2, the translation of $T^\varepsilon v^\varepsilon$ in time is controlled. To obtain equi-continuity with respect to translations in space, one needs to compare solutions from different cells and also within one cell which means we need to control these translations with respect to x and z. The strong convergence of $r(u^\varepsilon)$ to $r(u)$ in $L^2(0,T;L^2(\Gamma\times(0,1)))$ and the monotonicity of w^ε are essentially used to achieve this.

First, we consider the translation in x. To this aim, let η_x be a positive real number and

$$Q_{\eta_x} := \{(x,z) \in (0,1)\times(0,1) \mid \text{dist}\left((x,z), \partial((0,1)\times(0,1))\right) < \eta_x\}.$$

Then,

$$\tfrac{1}{2}\tfrac{d}{dt}\|\triangle_{\eta_x} T^\varepsilon v^\varepsilon\|^2_{L^2(Q_{\eta_x})} = \int\limits_{Q_{\eta_x}} \left(\triangle_{\eta_x} T^\varepsilon v^\varepsilon\right)\left(\triangle_{\eta_x} T^\varepsilon r(u^\varepsilon) - \triangle_{\eta_x} T^\varepsilon w^\varepsilon\right) dxdz.$$

Using the monotonicity of $T^\varepsilon w^\varepsilon$ with respect to $T^\varepsilon v^\varepsilon$, one has

$$\left(\triangle_{\eta_x} T^\varepsilon v^\varepsilon\right)\left(\triangle_{\eta_x} T^\varepsilon w^\varepsilon\right) \ge 0, \tag{32}$$

implying

$$\frac{1}{2}\frac{d}{dt}\|\triangle_{\eta_x} T^\varepsilon v^\varepsilon\|^2_{L^2(\Omega_{\eta_x})} \le \int\limits_{\Gamma\times\Omega_{\eta_x}} \left(\triangle_{\eta_x} T^\varepsilon v^\varepsilon\right)\left(\triangle_{\eta_x} T^\varepsilon r(u^\varepsilon)\right) dxdz \le \frac{1}{2}\|\triangle_{\eta_x} T^\varepsilon v^\varepsilon\|^2_{L^2(\Omega_{\eta_x})} + \frac{1}{2}\|\triangle_{\eta_x} T^\varepsilon r(u^\varepsilon)\|^2_{L^2(\Omega_{\eta_x})}.$$

As $|\eta_x| \searrow 0$ and due to the strong convergence of $T^\varepsilon r(u^\varepsilon)$, the second approaches 0 uniformly with respect to η_x (IV.26 in [9]). By Gronwall's lemma we conclude that

$$\|\triangle_{\eta_x} T^\varepsilon v^\varepsilon\|^2_{L^2(\Omega_{\eta_x})} \to 0 \text{ as } |\eta_x| \to 0$$

uniformly. For the translation with respect to z, we can proceed similarly; we omit the details. Further, the time translations are bounded since $\partial_t v^\varepsilon$ is bounded uniformly in ε. Therefore $T^\varepsilon v^\varepsilon$ converges strongly in $L^2(0,T;L^2(\Gamma\times(0,1)))$ (recall the convention referring to a subsequence). □

The only term to be considered is w^ε. Specifically, we have to identify its limit w as a member of $H(v)$. This is obtained in the following

Lemma 4.17 *With v and w being the limits of $T^\varepsilon v^\varepsilon$ and $T^\varepsilon w^\varepsilon$ one has $w \in H(v)$ a.e.*

Proof. The proof follows the ideas in proving Theorem 2.21 in [17], or Theorem 2.15 in [13], but now applied to the sequence of unfolded triples $(T^\varepsilon u^\varepsilon, T^\varepsilon v^\varepsilon, T^\varepsilon w^\varepsilon)$. We omit the details here.

□

4.4 Connecting the limits

In Lemma 4.7 we have obtained u_0 as the limit of u^ε restricted to Ω. Since $u_0 \in L^2(0,T;H^1(\Omega))$, we have the trace of u_0 defined at $\partial\Omega$. Next, we considered trace of u^ε defined on Γ^ε and constructed the periodically unfolding sequence $T^\varepsilon u^\varepsilon$ defined at $(0,T)\times\Gamma\times(0,1)$. We also proved in Lemma 4.14 that $T^\varepsilon u^\varepsilon$ converges strongly to u in $L^2((0,T)\times(0,1)\times\Gamma)$. It remains to connect these two limits and show that the trace of u_0 coincides with u. We prove this in the following Lemma.

Lemma 4.18 *It holds that*

$$\left\| u\left(t,x,(z,h(z))\right) - u_0\left(t,x,y=0\right)\right\|_{L^1(0,T;L^1((0,1)\times\Gamma))} = 0, \tag{33}$$

implying that the trace of u_0 and u (obtained as limit of $T^\varepsilon u^\varepsilon$) coincide a.e..

Proof. The choice of L^1 norm simplifies the computations. Let

$$\mathcal{I} := \int_0^T \int_0^1 \int_\Gamma \left| u\left(t,x,z\right) - u_0\left(t,x,y=0\right)\right| ds dx dt.$$

By using the triangle inequality we obtain

$$\begin{aligned}
\mathcal{I} \;\le\; & \int_0^T \int_0^1 \int_\Gamma \left| u\left(t,x,(z,h(z))\right) - T^\varepsilon u^\varepsilon\left(t,x,(z,h(z))\right)\right| ds dx dt \\
& + \int_0^T \int_0^1 \int_\Gamma \left| u^\varepsilon(t,\varepsilon\left\lfloor\frac{x}{\varepsilon}\right\rfloor + \varepsilon z, \varepsilon h(z)) - u^\varepsilon(t,\varepsilon\left\lfloor\frac{x}{\varepsilon}\right\rfloor + \varepsilon z, 0)\right| ds dx dt \\
& + \int_0^T \int_0^1 \int_\Gamma \left| u^\varepsilon(t,\varepsilon\left\lfloor\frac{x}{\varepsilon}\right\rfloor + \varepsilon z, 0) - u^\varepsilon(t,x,0)\right| ds dx dt \\
& + \int_0^T \int_0^1 \int_\Gamma \left| u^\varepsilon\left(t,x,y=0\right) - u_0\left(t,x,y=0\right)\right| ds dx dt.
\end{aligned}$$

Now we show that each of the term on the right, denoted by $\mathcal{I}_i, i = 1,\ldots,4$, converge to 0. Recalling Lemma 4.14, for the first term we have

$$\mathcal{I}_1 = \left\| u\left(t,x,(z,h(z))\right) - T^\varepsilon u^\varepsilon\left(t,x,h(z)\right)\right\|_{L^1((0,T)\times(0,1)\times\Gamma)} \to 0.$$

For $\mathcal{I}_2$, using Cauchy-Schwarz inequality gives

$$\mathcal{I}_2 = \int_0^T \int_0^1 \int_\Gamma \Big| \int_0^{\varepsilon h(z)} \partial_\xi u^\varepsilon \Big| \le \int_0^T \int_0^1 \int_\Gamma \left(\varepsilon |h|^{\frac{1}{2}} \int_0^{\varepsilon h} |\partial_z u^\varepsilon|^2 \right)^{\frac{1}{2}} \le C\varepsilon^{\frac{1}{2}} \|\partial_z u^\varepsilon\|_{L^2(\Omega^{\varepsilon T})} \le C\sqrt{\varepsilon} \|\nabla u^\varepsilon\|_{L^2(\Omega^{\varepsilon T})}.$$

The last term is bounded by $C\varepsilon^{\frac{1}{2}}$ because u^ε in $L^2(0,T;H^1(\Omega^\varepsilon))$. This implies that $\mathcal{I}_2 \searrow 0$ as $\varepsilon \searrow 0$.

The next term is the translation of u^ε by εz in the x direction. Since $|z| \le 1$, Lemma 4.12 gives

$$\mathcal{I}_3 \le C|\varepsilon|^{\frac{1}{2}},$$

approaching 0 as $\varepsilon \searrow 0$.

For the last term we find

$$\mathcal{I}_4 = \left\| u^\varepsilon\left(t,x,y=0\right) - u_0\left(t,x,y=0\right)\right\|_{L^1((0,T)\times(0,1)\times\Gamma)} = |\Gamma| \left\| u^\varepsilon\left(t,x,y=0\right) - u_0\left(t,x,y=0\right)\right\|_{L^1((0,T)\times(0,1))}.$$

In view of Lemma 4.7, this term converges to 0 as well, which concludes the proof. □

5 Limit equations: proof of Theorem 3.2

In this section, we establish the limit equations and hence prove Theorem 3.2. Since we have already established that the trace of u_0 is equal to u, the limit of $T^\varepsilon u^\varepsilon$, for notational convenience we denote both the limits u_0 and u by u. From the weak formulation, $(7)_1$, choose for $\phi \in H^1((0,T)\times\Omega),$ s.t. $\phi(T,x)=0$ to rewrite

$$-\int_0^T\int_\Omega u^\varepsilon(\partial_t\phi)dxdt+\int_0^T\int_\Omega \nabla u^\varepsilon\nabla\phi dxdt+\int_0^T\int_\Omega \mathbf{q}^\varepsilon u^\varepsilon\nabla\phi dxdt+\int_0^T\int_{\Gamma^\varepsilon}(\partial_t v^\varepsilon)\phi dxdt$$
$$=\int_\Omega u_I\phi(x,0)dxdt-\int_0^T\int_{\Omega^\varepsilon\setminus\Omega} u^\varepsilon(\partial_t\phi)dxdt+\int_{\Omega^\varepsilon\setminus\Omega} u_I\phi(x,0)dxdt-\int_0^T\int_{\Omega^\varepsilon\setminus\Omega}\left(\nabla u^\varepsilon\nabla\phi+\mathbf{q}^\varepsilon u^\varepsilon\nabla\phi\right)dxdt.$$

All terms on the left in the above have the to desired limits: for the first two terms, this follows from Lemma 4.7; for the third term we use (11) and the strong convergence of u^ε. For the boundary term we have

$$\lim_{\varepsilon\searrow 0}\int_0^T\int_{\Gamma^\varepsilon}(\partial_t v^\varepsilon)\phi dxdt=\int_0^T\int_{(0,1)\times\Gamma}(\partial_t v)\phi dxdsdt$$

using the weak convergence of $T^\varepsilon\partial_t v^\varepsilon$ shown in Lemma 4.10.

Furthermore, excepting the first integral, all terms on the right are integrals on $\Omega^\varepsilon\setminus\Omega$. Due to Lemma 4.9, all these integrals vanish, giving the desired limit equation.

Next, we consider the equation $(7)_2$. By a change of coordinate, this can be immediately rewritten as

$$\int_0^T\int_{(0,1)\times\Gamma}(\partial_t T^\varepsilon v^\varepsilon)(T^\varepsilon\theta)dxdsdt=\int_0^T\int_{(0,1)\times\Gamma}\left(T^\varepsilon r(u^\varepsilon)-T^\varepsilon w^\varepsilon\right)(T^\varepsilon\theta)dxdsdt$$

for all $\theta\in L^2(0,T;\Gamma^\varepsilon)$. Lemma 4.15 provides the strong convergence of $T^\varepsilon r^\varepsilon$; the weak convergence of $T^\varepsilon w^\varepsilon$ follows from Lemma 4.10, leading to

$$\int_0^T\int_{(0,1)\times\Gamma}(\partial_t v)\theta dxdsdt=\int_0^T\int_{(0,1)\times\Gamma}\left(r(u)-w\right)\theta dxdsdt$$

for all $\theta\in L^2(0,T;L^2((0,1)\times\Gamma))$.

Finally, $w\in H(v)$ thanks to Lemma 4.17, which completes the proof of Theorem 3.2.

6 Extensions to different rates

In this work, we have focussed on the proof for the crystal precipitation dissolution model involving a non-Lipschitz, possibly multi-valued rate. However, the techniques can be used to treat different reaction rates. In what follows, we provide two more examples of non-linear rates and comment upon the scheme of the proof. We spare the full details.

6.1 Model 1

We consider the following model

$$\partial_t u^\varepsilon-\Delta u^\varepsilon+\mathbf{q}^\varepsilon\nabla u^\varepsilon=0,\quad \text{in}\quad \Omega^{\varepsilon T} \tag{34}$$
$$\partial_t v^\varepsilon=r(u^\varepsilon)-g(v^\varepsilon),\quad \text{on}\quad \Gamma^{\varepsilon T} \tag{35}$$

and let us assume that r has the same structure given earlier. For g, we assume Lipschitz continuity and that it takes positive values. Such rates are considered for example in modeling the reactive flows in porous medium [24], in biological contexts in the diffusion of receptors in a cell [36], or in the description of sulphate attack for sewer pipes [19]. The extension to more number of species living on the boundary or inside the domain is analogous. For the model, the derivation of a priori estimates follows standard techniques. Since the reaction terms are Lipschitz, we obtain for $\partial_t u^\varepsilon\in L^2(0,T;L^2(\Omega^\varepsilon))$ (see e.g. [36]). We directly give the results and comment upon the particularities.

Theorem 6.1 *As $\varepsilon \searrow 0$, the pair $(u^\varepsilon, v^\varepsilon)$ converges to (u, v) and the limits satisfy the following equation defined in Ω^T*

$$\begin{aligned}(\partial_t u, \phi)_{\Omega^T} + (\nabla u, \nabla\phi)_{\Omega^T} - (\boldsymbol{q}u, \nabla\phi)_{\Omega^T} &= -(\partial_t v, \phi)_{(0,1)\times\Gamma\times(0,T)},\\ (\partial_t v, \theta)_{(0,T)\times(0,1)\times\Gamma} &= (r(u) - g(v), \theta)_{(0,1)\times\Gamma\times(0,T)}\end{aligned} \tag{36}$$

for all $(\phi, \theta) \in L^2(0, T; H^1_{0,\Gamma_D}(\Omega)) \times L^2(0, T \times (0, 1) \times \Gamma)$.

Remark 6.2 Compared to the proof of Theorem 3.2, the only difference is in obtaining the strong convergence of $T^\varepsilon v^\varepsilon$. We sketch briefly the steps involved in the proof for this strong convergence. We adopt the same framework as in the proof for Lemma 4.16 and re-do some of the steps of the proof for the translation in x. Let η_x be a positive real number and Q_{η_x} be an arbitrary compact subset of $(0, 1) \times (0, 1)$ as defined before. We have,

$$\tfrac{1}{2}\tfrac{d}{dt}\|\triangle_{\eta_x}(T^\varepsilon v^\varepsilon)\|^2_{L^2(Q_{\eta_x})} = \int\limits_{Q_{\eta_x}} \triangle_{\eta_x}(T^\varepsilon v^\varepsilon)\left(\triangle_{\eta_x}(T^\varepsilon r(u^\varepsilon)) - \triangle_{\eta_x}(T^\varepsilon g(v^\varepsilon))\right) dxdz$$

which leads to using Cauchy Schwarz and Young's inequality,

$$\tfrac{1}{2}\tfrac{d}{dt}\|\triangle_{\eta_x}T^\varepsilon v^\varepsilon\|^2_{L^2(\Gamma\times\Omega_{\eta_x})} \le (\tfrac{1}{2} + L_g)\|\triangle_{\eta_x}T^\varepsilon v^\varepsilon(x)\|^2_{L^2(\Omega_{\eta_x})} + \tfrac{1}{2}\|\triangle_{\eta_x}T^\varepsilon r(u^\varepsilon)\|^2_{L^2(\Omega_{\eta_x})}$$

where L_g is the Lipschitz constant of g. For the rest, the arguments remain the same. Note that as $|\eta_x| \searrow 0$, the strong convergence of $T^\varepsilon r(u^\varepsilon)$, implies that the second term goes to 0 uniformly with respect to η_x (IV.26 in [9]). Using Gronwall's lemma we conclude that the translations go to 0 as $|\eta_x| \searrow 0$. Similarly, the translation with respect to z is similarly treated which together establish the strong convergence of $T^\varepsilon v^\varepsilon$ in $L^2(0, T; L^2(\Gamma \times (0, 1)))$.

Remark 6.3 For the 2-scale convergence framework of periodic homogenization, the Lipschitz rate at the boundary is treated by the periodic unfolding techniques in [36]. There it is proved that $T^\varepsilon v^\varepsilon$ is a Cauchy sequence. Further, it is to be noted that the above proof also works if g is not Lipschitz but is only monotonic and bounded as is the case for the precipitation dissolution model considered here.

6.2 Model 2

We discuss another model with non-linear reaction rates that can be treated analogously.

$$\partial_t u^\varepsilon - \Delta u^\varepsilon + \mathbf{q}^\varepsilon\nabla u^\varepsilon = 0, \tag{37}$$

$$\partial_t v^\varepsilon = r(u^\varepsilon)(1 - sign^+(v^\varepsilon)) \tag{38}$$

where $sign^+(v^\varepsilon)$ is defined as

$$sign^+(v^\varepsilon) = \begin{cases} 1 & v^\varepsilon > 0,\\ 0 & v^\varepsilon \le 0.\end{cases} \tag{39}$$

and let us assume that r has the same structure given earlier. The model is considered in [7] describing the stiff dissolution rates in the context of the safe disposal of nuclear waste. In the cited reference, this problem is posed on core scale in a porous medium and analyzed numerically using the finite volume method. Here, we assume that the reactions take place at the rough boundaries and we are concerned with the upscaling of these rough boundary. The a priori estimates are again derived from standard techniques and we simply state the final result.

Theorem 6.4 *As $\varepsilon \searrow 0$, the pair $(u^\varepsilon, v^\varepsilon)$ converges to (u, v) and the limits satisfy the following equation defined in Ω^T*

$$\begin{aligned}(\partial_t u, \phi)_{\Omega^T} + (\nabla u, \nabla\phi)_{\Omega^T} - (\boldsymbol{q}u, \nabla\phi)_{\Omega^T} &= -(\partial_t v, \phi)_{(0,1)\times\Gamma\times(0,T)},\\ (\partial_t v, \theta)_{(0,T)\times(0,1)\times\Gamma} &= (r(u) - sign^+(v)r(u), \theta)_{(0,1)\times\Gamma\times(0,T)}\end{aligned} \tag{40}$$

for all $(\phi, \theta) \in L^2(0, T; H^1_{0,\Gamma_D}(\Omega)) \times L^2((0, T) \times (0, 1) \times \Gamma)$.

Remark 6.5 Once again the steps in the proof are analogous and we skip them. Note that once we have proved the strong convergence of $T^\varepsilon r^\varepsilon$ and $T^\varepsilon v^\varepsilon$, we are able to pass to the limit as this implies, $T^\varepsilon v^\varepsilon \to v$ pointwise a.e. with v bounded. The proof for strong convergence of $T^\varepsilon r^\varepsilon$ is same as in the above case. We remark on the difference in the proof for the strong convergence of $T^\varepsilon v^\varepsilon$. Adopting the same framework as in the proof for Lemma 4.16. Let Q_{η_x} be an arbitrary compact subset of $(0, 1) \times (0, 1)$ and let $\eta_x \in (0, dist(Q_{\eta_x}, \partial((0, 1) \times (0, 1))))$. We have,

$$\tfrac{1}{2}\tfrac{d}{dt}\|\triangle_{\eta_x}T^\varepsilon v^\varepsilon\|^2_{L^2(Q_{\eta_x})} = \int\limits_{Q_{\eta_x}} (\triangle_{\eta_x}T^\varepsilon v^\varepsilon)\triangle_{\eta_x}\left(T^\varepsilon r^\varepsilon(1 - T^\varepsilon sign^+(v^\varepsilon))\right) dxdz.$$

Note that the right hand side can be rewritten as

$$\triangle_{\eta_x}\left(T^\varepsilon r^\varepsilon(1-T^\varepsilon sign^+(v^\varepsilon))\right) = \triangle_{\eta_x}T^\varepsilon(r^\varepsilon)(1-T^\varepsilon sign^+(v^\varepsilon)) \\ +T^\varepsilon r(u^\varepsilon)\triangle_{\eta_x}(1-T^\varepsilon sign^+(v^\varepsilon))$$

and by the monotonicity (monotonically decreasing) of $1-T^\varepsilon sign^+(v^\varepsilon)$ and positivity of r, we have

$$T^\varepsilon r(u^\varepsilon)\triangle_{\eta_x}(1-T^\varepsilon sign^+(v^\varepsilon))\triangle_{\eta_x}T^\varepsilon v^\varepsilon \leq 0.$$

Using Cauchy Schwarz and Young's inequality, this gives

$$\tfrac{d}{dt}\|\triangle_{\eta_x}T^\varepsilon v^\varepsilon\|^2_{L^2(\Gamma\times\Omega_{\eta_x})} \leq \|\triangle_{\eta_x}T^\varepsilon v^\varepsilon\|^2_{L^2(\Omega_{\eta_x})} + \|\triangle_{\eta_x}T^\varepsilon r(u^\varepsilon)\|^2_{L^2(\Omega_{\eta_x})}.$$

Following the argument that as $|\eta_x| \searrow 0$, the strong convergence of $T^\varepsilon r(u^\varepsilon)$ implies that the second term goes to 0 uniformly with respect to η_x (IV.26 in [9]). Using Gronwall's lemma then concludes the proof.

7 Numerical simulations

To study the approximation of the upscaled equations to the original equations, we make the following choices for the geometry. To construct Ω^ε, we make the following choice for Γ^ε:

$$\Gamma^\varepsilon = \{(x,y) : x \in (0,1)\ y = -1.1\varepsilon + \varepsilon\sin(\pi/2 + 2\pi\frac{x}{\varepsilon})\}$$

which makes sure that $\Omega \subset \Omega^\varepsilon$ and we conduct the numerical experiments for different ε. For the flow, we solve the Stokes equation for Ω^ε domain with parabolic inlet profile and for Ω we have the exact solution $\mathbf{q} = 6y(1-y)\mathbf{e}_1$. For the choice of reaction rates, we choose for precipitation,$r(u) = [u]_+$, and for dissolution rate, we choose the regularized Heaviside function

$$H_\delta(v^\varepsilon) := \begin{cases} 1, & v^\varepsilon > \delta, \\ \frac{v^\varepsilon}{\delta}, & 0 \leq v^\varepsilon \leq \delta, \\ 0, & v^\varepsilon < 0 \end{cases} \tag{41}$$

and we choose for $\delta = 0.01$. The choice of this regularized Heaviside function has been already investigated for numerical analysis and we refer to [13] for the details.
For the computations, we use finite element method with BDF time stepping for solving the equations as implemented in the COMSOL Multiphysics package [25].

We choose the following initial conditions:

$$u^\varepsilon(x,y,t=0) = 1, \quad \text{in} \quad \Omega^\varepsilon, \quad v^\varepsilon(x,t=0) = 0.2 \quad \text{on} \quad \Gamma^\varepsilon;$$

and for u, v also we choose

$$u(x,y,t=0) = 1, \quad \text{in} \quad \Omega, \quad v(x,t=0) = 0.2 \quad \text{on} \quad y=0,\ x \in (0,1).$$

Note that for this choice of v^ε, v we have $r(u^\varepsilon) - H_\delta(v^\varepsilon) = r(u) - H_\delta(v) = 0$ and hence $\partial_t v^\varepsilon = \partial_t v = 0$ leading to the equilibrium situation. According to different boundary conditions imposed at $x = 0$, we consider the following situations.

7.1 Dissolution fronts

We perturb the equilibrium at $x = 0$ by imposing the boundary condition $u^\varepsilon = u = 0$. Due to this the dissolution starts taking place as $\partial_t v^\varepsilon, \partial_t v < 0$ at $x = 0$. This gives rise to the dissolution fronts and these fronts proceed to the right as time progresses. We study this case for different choices of ε.

7.1.1 Concentration at the boundary

We compute the full solution for different ε and plot u^ε and u at the boundary Γ^ε and $y = 0$ boundary of Ω respectively at $t = 0.5$. The plot is shown in Figure 2. Due to the oscillations in the boundary the maximum error takes place at the boundary itself. We compute the concentration at the oscillating boundary for given ε and then plot it against the upscaled concentration u at $y = 0$. Because of the oscillating boundary, the concentration has an oscillating profile while the upscaled concentration has a monotonic profile; however, as ε decreases, u^ε converges to u.
For v^ε, the corresponding plot is shown in Figure 3. For small ε we see that the upscaled profile provides a good approximation for the full solution. Further, as ε decreases, the v^ε converges to v.

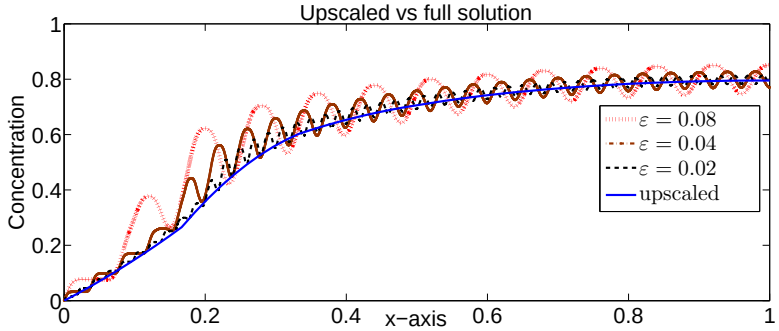

Fig. 2 Concentration profiles for dissolution process at the boundary for different ε at $t = 0.5$.

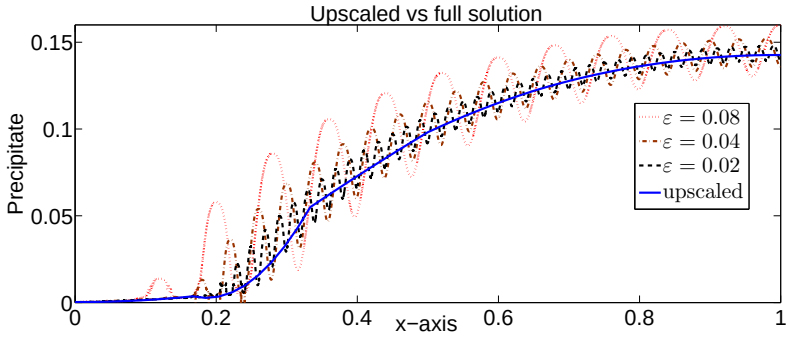

Fig. 3 Precipitate concentration profiles for dissolution process at the boundary for different ε at $t = 0.5$.

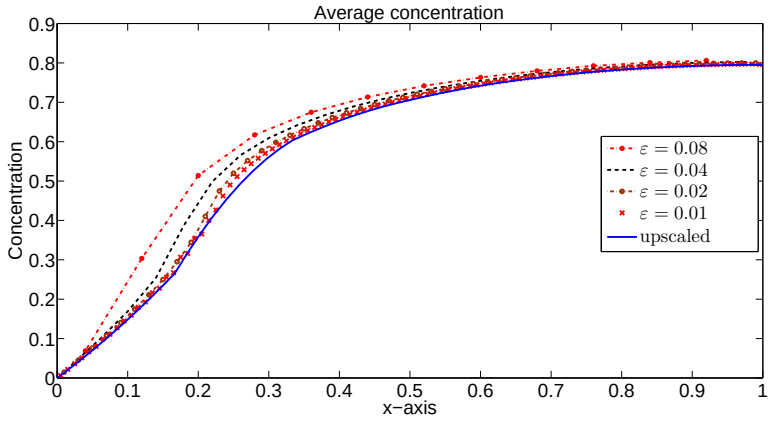

Fig. 4 Average concentration $\bar{u}$ for dissolution process for different ε at $t = 0.5$.

7.1.2 Error at the boundary

Next, we consider the $L^2(\Gamma_1), \Gamma_1 := \{(x, 0)|x \in (0, 1)\}$ error at the boundary at $t = 0.5$. Specifically, we assume that the error is of order ε^{α_u},

$$E_\varepsilon^u := \|u^\varepsilon - u\|_{L^2(\Gamma_1)} \leq C\varepsilon^{\alpha_u}.$$

To estimate α_u, we compute the error for various values of ε and determine the ratio

$$\alpha_u(i) = \frac{\log(\text{error(i)}) - \log(\text{error(i} - 1))}{\log(\varepsilon(i)) - \log(\varepsilon(i-1))}, \quad i = 2, \ldots, 6.$$

ε	0.1000	0.0800	0.0500	0.0400	0.0200	0.0100
error	0.1118	0.0844	0.0516	0.0453	0.0218	0.0106
α_u		0.9195	0.9746	1.1003	0.9588	0.9754

Table 1 Table for L^2 error for the concentrations.

In Table 1 we give the values of the error as well as the convergence rate α_u computed from the preceding formula. The convergence order is close to 1.
Similarly, for v^ε we assume the convergence order α_v and compute

$$E_\varepsilon^v := \|v^\varepsilon - v\|_{L^2(\Gamma_1)} \leq C\varepsilon^{\alpha_v}.$$

The results are tabulated in Table 2. As it is seen below, the convergence order is better than 1.

ε	0.1000	0.0800	0.0500	0.0400	0.0200	0.0100
error	0.0268	0.0206	0.0125	0.0114	0.0061	0.0030
α_v		1.3000	1.3725	1.4783	1.3403	1.2582

Table 2 Table for L^2 error for the precipitate concentration.

We now compare the average concentration at the boundary. We define

$$\bar{u}(x) := \frac{1}{\varepsilon}\int_{\varepsilon\lfloor\frac{x}{\varepsilon}\rfloor-\frac{\varepsilon}{2}}^{\varepsilon\lfloor\frac{x}{\varepsilon}\rfloor+\frac{\varepsilon}{2}} u^\varepsilon ds$$

Observe that $\bar{u}$ provides information regarding the average concentration into one periodic unit for ε model. We compare this with the upscaled equation in Figure 4. The agreement is very good for small ε which indicates the quality of upscaling.

7.2 Precipitation process

Next, we again choose the same initial condition as above and we study the precipitation process by imposing the boundary condition

$$u^\varepsilon = u = 2, \quad \text{at} \quad x = 0$$

and with this choice, note that $\partial_t v^\varepsilon, \partial_t v > 0$ and hence the precipitation process starts taking place. This leads to an increase in v^ε, v as time progresses and for u^ε, u a steady state is achieved. We show the solutions for different ε and we compute the full solution for $\varepsilon = 0.1, 0.02$ and plot u^ε and u at the boundary Γ^ε and $y = 0$ boundary of Ω respectively at $t = 1$. The corresponding plots for u^ε and v^ε are shown in Figure 5, respectively in 6. Again, due to the oscillations in the boundary, we have the boundary layer and the maximum error takes place at the boundary itself. We compute the concentration at the oscillating boundary for given ε and then plot it against the upscaled concentration u at $y = 0$. Because of the oscillating boundary, the concentration has an oscillating profile while the upscaled concentration has a monotonic profile; however, as ε decreases, $u^\varepsilon, v^\varepsilon$ converges to u, v.

8 Conclusions

We have rigorously derived the upscaled model for the crystal precipitation dissolution model defined in a domain with rough/oscillating boundary characterized by period and amplitude ε. The upscaled model is obtained as the limit of sequence $\varepsilon \searrow 0$. The derivation uses the homogenization arguments where we use the periodic unfolding techniques to use the desired compactness arguments. The non-linear reaction rates in particular the multi-valued dissolution rates require stronger convergence properties for passing to the limit which is achieved by considering translation estimates. Even though the derivation here has been specific to the precipitation-dissolution model, similar techniques may be used for a different kinds of reaction rates. We have given some specific examples of such rates. Moreover, we have provided numerical computations to show the convergence. We see that the upscaled solutions approximate the full solution very well and hence provide a convincing argument for the usefulness of upscaling techniques.

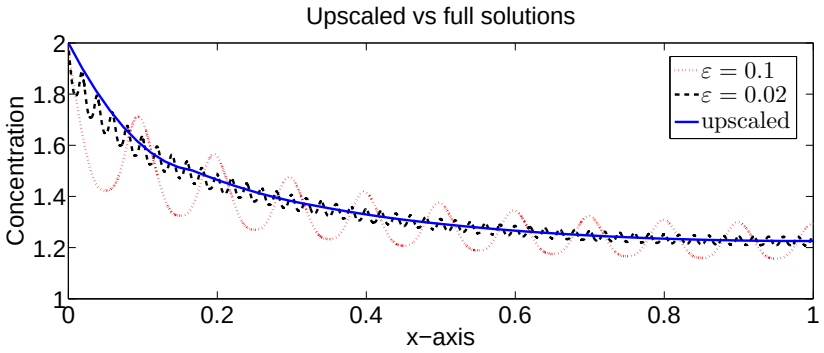

Fig. 5 Concentration profiles at the boundary for different ε at $t = 1$ (precipitation).

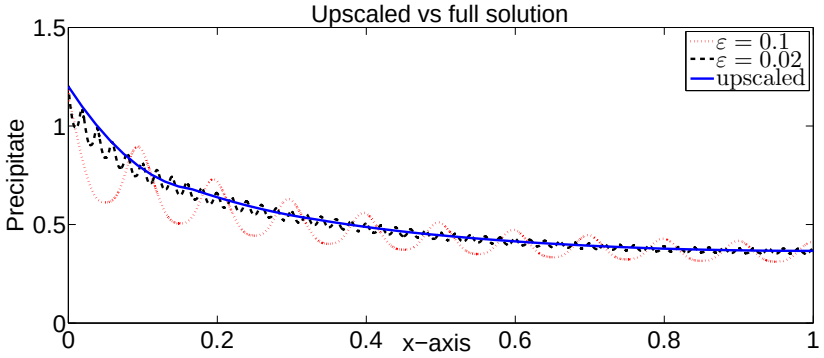

Fig. 6 Precipitate concentration at the boundary for different ε at $t = 1$ (precipitation).

Acknowledgement

The work of K. Kumar was supported by STW project no. 07796. The support is gratefully acknowledged. Part of the work was completed when M. van Helvoort was visiting the Institute for Hydraulic Engineering, University of Stuttgart, supported by the International Research Training Group NUPUS (GRK 1398) and The Netherlands Organisation for Scientific Research (DN 81-754). The authors would like to thank Prof. M.A. Peletier (Eindhoven) for the suggestions concerning Lemma 4.12, to Prof. R. Helmig (Stuttgart), Prof. P. Notten (Eindhoven) and Mrs. T. Fatima (Eindhoven) for the valuable suggestions concerning the subject and the content of the paper.

References

[1] G. Allaire. Homogenization and two-scale convergence. *SIAM J. Math. Anal.*, 23(6):1482–1518, 1992.
[2] G. Allaire and M. Amar. Boundary layer tails in periodic homogenization. *ESAIM Control Optim. Calc. Var.*, 4:209–243 (electronic), 1999.
[3] J. M. Arrieta and S. M. Bruschi. Very rapidly varying boundaries in equations with nonlinear boundary conditions. The case of a non uniformly Lipschitz deformation. *Discrete Contin. Dyn. Syst. Ser. B*, 14(2):327–351, 2010.
[4] J. M. Arrieta and M. C. Pereira. Elliptic problems in thin domains with highly oscillating boundaries. *Bol. Soc. Esp. Mat. Apl. SẽMA*, (51):17–24, 2010.
[5] J. M. Arrieta and M. C. Pereira. Homogenization in a thin domain with an oscillatory boundary. *J. Math. Pures Appl. (9)*, 96(1):29–57, 2011.
[6] J. F. Bonder, R. Orive, and J. D. Rossi. The best Sobolev trace constant in a domain with oscillating boundary. *Nonlinear Anal.*, 67(4):1173–1180, 2007.
[7] N. Bouillard, R. Eymard, R. Herbin, and P. Montarnal. Diffusion with dissolution and precipitation in a porous medium: mathematical analysis and numerical approximation of a simplified model. *M2AN Math. Model. Numer. Anal.*, 41(6):975–1000, 2007.
[8] A. Bourgeat, S. Luckhaus, and A. Mikelić. Convergence of the homogenization process for a double-porosity model of immiscible two-phase flow. *SIAM J. Math. Anal.*, 27(6):1520–1543, 1996.
[9] H. Brezis. *Analyse fonctionnelle*. Collection Mathématiques Appliquées pour la Maîtrise. [Collection of Applied Mathematics for the Master's Degree]. Masson, Paris, 1983. Théorie et applications. [Theory and applications].

[10] G. A. Chechkin, A. Friedman, and A. L. Piatnitski. The boundary-value problem in domains with very rapidly oscillating boundary. *J. Math. Anal. Appl.*, 231(1):213–234, 1999.

[11] D. Cioranescu, A. Damlamian, and G. Griso. The periodic unfolding method in homogenization. *SIAM J. Math. Anal.*, 40(4):1585–1620, 2008.

[12] A. Damlamian and K. Pettersson. Homogenization of oscillating boundaries. *Discrete Contin. Dyn. Syst.*, 23(1-2):197–219, 2009.

[13] V. M. Devigne, I. S. Pop, C. J. van Duijn, and T. Clopeau. A numerical scheme for the pore-scale simulation of crystal dissolution and precipitation in porous media. *SIAM J. Numer. Anal.*, 46(2):895–919, 2008.

[14] C. J. van Duijn and P. Knabner. Solute transport through porous media with slow adsorption. In *Free boundary problems: theory and applications, Vol. I (Irsee, 1987)*, volume 185 of *Pitman Res. Notes Math. Ser.*, pages 375–388. Longman Sci. Tech., Harlow, 1990.

[15] C. J. van Duijn and P. Knabner. Solute transport in porous media with equilibrium and nonequilibrium multiple-site adsorption: travelling waves. *J. Reine Angew. Math.*, 415:1–49, 1991.

[16] C. J. van Duijn and P. Knabner. Travelling wave behaviour of crystal dissolution in porous media flow. *European J. Appl. Math.*, 8(1):49–72, 1997.

[17] C. J. van Duijn and I. S. Pop. Crystal dissolution and precipitation in porous media: pore scale analysis. *J. Reine Angew. Math.*, 577:171–211, 2004.

[18] L. C. Evans. *Partial differential equations*, volume 19 of *Graduate Studies in Mathematics*. American Mathematical Society, Providence, RI, 1998.

[19] T. Fatima, N. Arab, E. P. Zemskov, and A. Muntean. Homogenization of a reaction-diffusion system modeling sulfate corrosion of concrete in locally periodic perforated domains. *J. Engrg. Math.*, 69(2-3):261–276, 2011.

[20] A. Friedman and B. Hu. A non-stationary multi-scale oscillating free boundary for the Laplace and heat equations. *J. Differential Equations*, 137(1):119–165, 1997.

[21] A. Friedman, B. Hu, and Y. Liu. A boundary value problem for the Poisson equation with multi-scale oscillating boundary. *J. Differential Equations*, 137(1):54–93, 1997.

[22] U. Hornung. Introduction: homogenization and porous media. pages 1–25, 1997.

[23] U. Hornung and W. Jäger. Diffusion, convection, adsorption, and reaction of chemicals in porous media. *J. Differential Equations*, 92(2):199–225, 1991.

[24] U. Hornung, W. Jäger, and A. Mikelić. Reactive transport through an array of cells with semi-permeable membranes. *RAIRO Modél. Math. Anal. Numér.*, 28(1):59–94, 1994.

[25] COMSOL Inc. `http://www.comsol.com`.

[26] W. Jäger and A. Mikelić. On the boundary conditions at the contact interface between a porous medium and a free fluid. *Ann. Scuola Norm. Sup. Pisa Cl. Sci. (4)*, 23(3):403–465, 1996.

[27] W. Jäger and A. Mikelić. On the interface boundary condition of Beavers, Joseph, and Saffman. *SIAM J. Appl. Math.*, 60(4):1111–1127 (electronic), 2000.

[28] W. Jäger and A. Mikelić. On the roughness-induced effective boundary conditions for an incompressible viscous flow. *J. Differential Equations*, 170(1):96–122, 2001.

[29] P. Knabner, C. J. van Duijn, and S. Hengst. An analysis of crystal dissolution fronts in flows through porous media. part 1: Compatible boundary conditions. *Adv. Water Resour.*, 18:171–185, 1995.

[30] K. Kumar, M. Neuss-Radu, and I. S. Pop. Homogenization of crystal precipitation and dissolution model in a porous medium. *In Preparation*, 2012.

[31] K. Kumar, T. L. van Noorden, and I. S. Pop. Effective dispersion equations for reactive flows involving free boundaries at the microscale. *Multiscale Model. Simul.*, 9, 2011.

[32] K. Kumar, T.L. van Noorden, and I.S. Pop. Upscaling of reactive flows in domains with moving oscillating boundaries. *CASA Report 12-12*, 2012.

[33] K. Kumar, I. S. Pop, and F. A. Radu. Convergence analysis for a conformal discretization of a model for precipitation and dissolution in porous media. *CASA Report 12-08*, 2012.

[34] K. Kumar, I. S. Pop, and F. A. Radu. Convergence analysis of mixed numerical schemes for reactive flow in a porous medium. *CASA Report 12-20*, 2012.

[35] J.-L. Lions and E. Magenes. *Non-homogeneous boundary value problems and applications. Vol. I*. Springer-Verlag, New York, 1972. Translated from the French by P. Kenneth, Die Grundlehren der mathematischen Wissenschaften, Band 181.

[36] A. Marciniak-Czochra and M. Ptashnyk. Derivation of a macroscopic receptor-based model using homogenization techniques. *SIAM J. Math. Anal.*, 40(1):215–237, 2008.

[37] N. Neuss, M. Neuss-Radu, and A. Mikelić. Effective laws for the Poisson equation on domains with curved oscillating boundaries. *Appl. Anal.*, 85(5):479–502, 2006.

[38] M. Neuss-Radu. Some extensions of two-scale convergence. *C. R. Acad. Sci. Paris Sér. I Math.*, 322(9):899–904, 1996.

[39] M. Neuss-Radu and W. Jäger. Effective transmission conditions for reaction-diffusion processes in domains separated by an interface. *SIAM J. Math. Anal.*, 39(3):687–720 (electronic), 2007.

[40] G. Nguetseng. A general convergence result for a functional related to the theory of homogenization. *SIAM J. Math. Anal.*, 20(3):608–623, 1989.

[41] T. L. van Noorden. Crystal precipitation and dissolution in a porous medium: effective equations and numerical experiments. *Multiscale Model. Simul.*, 7(3):1220–1236, 2008.

[42] T. L. van Noorden. Crystal precipitation and dissolution in a thin strip. *European J. Appl. Math.*, 20(1):69–91, 2009.

[43] T. L. van Noorden and I. S. Pop. A Stefan problem modelling crystal dissolution and precipitation. *IMA J. Appl. Math.*, 73(2):393–411, 2008.

[44] T. L. van Noorden, I. S. Pop, and M. Röger. Crystal dissolution and precipitation in porous media: L^1-contraction and uniqueness. *Discrete Contin. Dyn. Syst.*, (Dynamical Systems and Differential Equations. Proceedings of the 6th AIMS International Conference, suppl.):1013–1020, 2007.

PREVIOUS PUBLICATIONS IN THIS SERIES:

Number	Author(s)	Title	Month
12-33	G. Ali N. Banagaaya W.H.A. Schilders C. Tischendorf	Index-aware model order reduction for index-2 differential-algebraic equations	Oct. '12
12-34	M. Pisarenco J.M.L. Maubach I.D. Setija R.M.M. Mattheij	Efficient solution of Maxwell's equations for geometries with repeating patterns by an exchange of discretization directions in the aperiodic Fourier modal method	Oct. '12
12-35	J.H.M. Evers S. Hille A. Muntean	Solutions to a measured-valued mass evolution problem with flux boundary conditions inspired by crowd dynamics	Oct. '12
12-36	L. Gulikers J.H.M. Evers A. Muntean A. Lyulin	The effect of perception anisotropy on particle systems describing pedestrian flows in corridors	Oct. '12
12-37	K. Kumar M. van Helvoort I.S. Pop	Rigorous upscaling of rough boundaries for reactive flows	Oct. '12

Ontwerp: de Tantes,
Tobias Baanders, CWI